Observer-Based Control of Piecewise-Affine Systems *

Luis Rodrigues†
Dept. of Aeronautics and Astronautics
Stanford University
Email: luisrod@stanford.edu

Jonathan P. How‡
Dept. of Aeronautics and Astronautics
Massachusetts Institute of Technology
Email: jhow@mit.edu

October 18, 2002

Abstract

This paper presents a new synthesis method for both state and dynamic output feedback control of a class of hybrid systems called piecewise-affine (PWA) systems. The synthesis procedure delivers stabilizing controllers that can be proven to give either asymptotic or exponential convergence rates. The synthesis method builds on existing PWA stability analysis tools by transforming the design into a closed-loop analysis problem wherein the controller parameters are unknown. More specifically, the proposed technique formulates the search for a piecewise-quadratic control Lyapunov function and a piecewise-affine control law as an optimization problem subject to linear constraints and a bilinear matrix inequality. The linear constraints in the synthesis guarantee that sliding modes are not generated at the switching. The resulting optimization problem is known to be $\mathcal{NP}$ hard, but suboptimal solutions can be obtained using the three iterative algorithms presented in the paper. The new synthesis technique allows controllers to be designed with a specified structure, such as a combined regulator and observer. The observers in these controllers then enable switching based on state estimates rather than on measured outputs. The overall design approach, including a comparison of the synthesis algorithms and the performance of the resulting controllers, is clearly demonstrated in four simulation examples.

*Paper provisionally accepted for publication in the *International Journal of Control.*
†Funded in part by a PRAXIS XXI grant.
‡Author to whom all correspondence should be addressed: 37-391, 77 Massachusetts Ave., Cambridge, MA 02319. Tel: (617) 253-3267; Fax: (617) 258-5940.

1 Introduction

Hybrid systems include both continuous-time and discrete-event components, and are an important modeling class for many applications. For example, the dynamics of many industrial processes can be modeled as evolving in continuous-time at the lower level (of the physical system) being driven by discrete-event logical components that impose mode switching at the higher level. Piecewise-affine (PWA) systems are a special class of hybrid systems in that the continuous dynamics within each discrete mode are affine and the mode switching always occurs at very specific subsets of the state space that are known *a-priori*. PWA systems are also an important modeling class for nonlinear systems because a wide variety of nonlinearities are either piecewise-affine (*e.g.,* a saturated linear actuator characteristic) or can be approximated as piecewise-affine functions [Johansson and Rantzer, 2000, Julián, 1999, Rodrigues and How, 2001, Hassibi *et al.*, 1999a]. In fact, piecewise-affine systems are a broad modeling class in the sense that they have been shown to be equivalent to many other classes of systems, such as mixed logic dynamical systems [Bemporad and Morari, 1999] and extended linear complementary systems [Schutter and Moor, 1999]. PWA systems thus represent an important starting point in the study of both hybrid and nonlinear systems. As such, this paper presents a new synthesis method for both state and dynamic output feedback controllers for PWA systems.

The roots of piecewise-affine systems date back to the pioneering works of Andronov [Andronov and Chaikin, 1949] on oscillations in nonlinear systems and Kalman [Kalman, 1954] on saturated linear systems. The practical relevance of piecewise-linear servomechanisms is also discussed in [Schwartz, 1953]. Although some research in the 1960's included piecewise-linear systems as a special case (*e.g.,* the work on absolute stability [Popov, 1961]) it was not until the 1970's that piecewise-affine systems were considered as a class of system models by the circuit theory community [Chua, 1977, Bokhoven, 1981]. In fact, piecewise-affine approximations of nonlinear circuit components were used frequently and the need to efficiently simulate and analyze large-scale circuits highlighted new research directions in the modeling, simulation, and analysis of piecewise-affine systems. In the early 1980's, Sontag [Sontag, 1981] presented a pioneering work on the analysis of discrete-time piecewise-linear systems. Similar ideas were used more recently to analyze the robustness of PWA systems [Kantner, 1997]. For continuous-time dynamics, a technique based on vector field considerations was developed by Pettit [Pettit, 1995] to provide a qualitative analysis of piecewise-linear systems.

Note that the analysis of even some simple piecewise-affine systems has been recently shown to be either an $\mathcal{NP}$ hard problem or undecidable [Blondel and Tsitsiklis, 1999].

Therefore, it is not expected that the analysis of PWA systems can be solved exactly using efficient algorithms with polynomial-time complexity. However, by searching for a Lyapunov function to prove stability, approximate analysis methods can be developed that can be formulated as convex optimization programs involving linear matrix inequalities (LMIs) [Boyd *et al.*, 1994]. These mathematical programs can then be solved efficiently using polynomial-time algorithms [Nesterov and Nemirovsky, 1994]. The methods are only approximate in the sense that there are no guarantees that a Lyapunov function can be found. However, if one is found, the result is unambiguous. This has been the trend of research on the linear parameter varying approach to gain scheduling (see [Rugh and Shamma, 2000] and references therein) and on the more recent work on the analysis of piecewise-affine systems based on Lyapunov functions and LMIs [Peleties and DeCarlo, 1991, Branicky, 1996, DeCarlo *et al.*, 2000, Johansson and Rantzer, 1998a, Pettersson, 1999, Hassibi and Boyd, 1998, Gonçalves *et al.*, 2001].

A first attempt to apply Lyapunov-based methods to piecewise-affine systems can be found in the work on switched linear systems initiated in [Peleties and DeCarlo, 1991]. Following this work, and its extensions to nonlinear dynamics [Branicky, 1996], a unified approach to the analysis of PWA systems and a class of hybrid systems was formulated in [DeCarlo *et al.*, 2000]. Based on this research, several Lyapunov-based methods have recently been developed to analyze piecewise-linear and piecewise-affine systems [Johansson and Rantzer, 1998a, Pettersson, 1999, Hassibi and Boyd, 1998, Gonçalves *et al.*, 2001]. Synthesis methods [Johansson and Rantzer, 2000, Hassibi and Boyd, 1998, Sluphaug, 1999] have also been developed using convex optimization programs based on the analysis methods in [Johansson and Rantzer, 1998a, Pettersson, 1999, Hassibi and Boyd, 1998]. The continuous-time controllers resulting from these approaches are either a patched LQR [Johansson and Rantzer, 2000] or they can not guarantee that sliding modes are avoided [Johansson and Rantzer, 2000, Hassibi and Boyd, 1998] and, therefore, are not provably stabilizing. Furthermore none of the approaches in [Johansson and Rantzer, 2000, Hassibi and Boyd, 1998, Sluphaug, 1999] address the output feedback problem. A key issue that must be addressed in output feedback controllers is how to perform state estimation for piecewise-affine systems. A new estimation algorithm for a class of hybrid systems has recently been presented in [Sworder and Boyd, 1999b, Sworder and Boyd, 1999a]. Their approach is based on gain-scheduling ideas as applied to jump linear systems. However, the approach applies to systems that have distinct measurements of the plant output and the switching parameters. Output feedback has recently been developed for discrete-time piecewise-affine systems in [Ferrari-Trecate *et al.*, 2000, Bemporad *et al.*, 2000, Imsland *et al.*, 2001].

Following the research initiated in [Rodrigues *et al.*, 2000], the current paper presents a Lyapunov-based approach to the design of a regulator and an observer for piecewise-affine continuous-time systems that do not necessarily have measurements of the switching parameters. Advantages of this design approach are that it provides a controller, a Lyapunov function that proves stability, and it enables switching based on the estimated states rather than on measured parameters. It also delivers controllers that are guaranteed to avoid sliding modes at the switching and that are either asymptotically or exponentially stable. It will be shown in this paper that the formulated control problem is a bi-convex optimization program, which can be solved iteratively for a suboptimal solution using efficient, polynomial-time algorithms at each iteration. Three different solution algorithms are presented. The effectiveness of the design technique is demonstrated in four examples covering a broad class of different engineering applications.

The paper is organized as follows. The system description and trajectory definition are presented first, which are followed by the formulation of the piecewise-affine (state and dynamic output) feedback synthesis as an optimization problem. Three algorithms for solving this problem for a suboptimal solution are described in Section 3.3, followed by four examples. One of the examples compares two of the proposed solution algorithms to show that they yield similar solutions to the control optimization problem in that case.

2 System Description and Trajectory Definition

It is assumed that a piecewise-affine system and a corresponding partition of the state space with polytopic cells $\mathcal{R}_i$, $i \in \mathcal{I} = \{1, \ldots, M\}$ are given (see [Rodrigues and How, 2001] for generating such a partition). Following [Johansson and Rantzer, 1998a, Pettersson, 1999, Hassibi and Boyd, 1998], each cell is constructed as the intersection of a finite number (p_i) of half spaces

$$\mathcal{R}_i = \{x \mid H_i^T x - g_i < 0\}, \tag{1}$$

where $H_i = [h_{i1} \;\; h_{i2} \ldots h_{ip_i}]$, $g_i = [g_{i1} \;\; g_{i2} \ldots g_{ip_i}]^T$. Moreover the sets $\mathcal{R}_i$ partition a subset of the state space $\mathcal{X} \subset I\!R^n$ such that $\cup_{i=1}^M \overline{\mathcal{R}}_i = \mathcal{X}$, $\mathcal{R}_i \cap \mathcal{R}_j = \emptyset$, $i \neq j$, where $\overline{\mathcal{R}}_i$ denotes the closure of $\mathcal{R}_i$. Within each cell the dynamics are affine and strictly proper of the form

$$\begin{aligned} \dot{x}(t) &= A_i x(t) + b_i + B_i u(t), \\ y(t) &= C_i x(t), \end{aligned} \tag{2}$$

where $x(t) \in \mathbb{R}^n$, $u(t) \in \mathbb{R}^m$, $y(t) \in \mathbb{R}^p$. Each polytopic cell has a finite number of facets and vertices. Any two cells sharing a common facet will be called *level-1* neighboring cells. Any finite number of cells sharing a common vertex will be called *level-2* neighboring cells. Let $\mathcal{N}_i = \{$*level*-1 neighboring cells of $\mathcal{R}_i\}$. It is also assumed that vectors $c_{ij} \in \mathbb{R}^n$ and scalars d_{ij} exist such that the facet boundary between cells $\mathcal{R}_i$ and $\mathcal{R}_j$ is contained in the hyperplane described by $\{x \in \mathbb{R}^n \,|\, c_{ij}^T x - d_{ij} = 0\}$, for $i = 1, \ldots, M$, $j \in \mathcal{N}_i$. A parametric description of the boundaries can then be obtained as [Hassibi and Boyd, 1998] (see figure 1)

$$\overline{\mathcal{R}_i} \cap \overline{\mathcal{R}_j} \subseteq \{l_{ij} + F_{ij} s \,|\, s \in \mathbb{R}^{n-1}\} \tag{3}$$

for $i = 1, \ldots, M$, $j \in \mathcal{N}_i$, where $F_{ij} \in \mathbb{R}^{n \times (n-1)}$ (full rank) is the matrix whose columns span the null space of c_{ij}, and $l_{ij} \in \mathbb{R}^n$ is given by $l_{ij} = c_{ij} \left(c_{ij}^T c_{ij}\right)^{-1} d_{ij}$.

[Figure 1 about here.]

Remark 1 Whenever $\mathcal{R}_i$ can be outer approximated by a finite union of (possibly degenerate) ellipsoids ε_{ij} for $j = 1, \ldots, J_i$, this covering can also be used to describe the regions (see [Hassibi and Boyd, 1998] for details). Although conservative, this description is useful because it often requires fewer parameters than the polytopic description. □

For system (2), we adopt the following definition of trajectories or solutions presented in [Johansson, 1999].

Definition 2.1 [Johansson, 1999] *Let $x(t) \in \mathcal{X}$ be an absolutely continuous function. Then $x(t)$ is a trajectory of the system (2) on $[t_0, t_f]$ if, for almost all $t \in [t_0, t_f]$ and Lebesgue measurable $u(t)$, the equation $\dot{x}(t) = A_i x(t) + b_i + B_i u(t)$ holds for $x(t) \in \overline{\mathcal{R}_i}$.* □

3 Controller Synthesis

The control design concept for piecewise-affine systems is depicted in figure 2. It is assumed that the control objective is to stabilize the system to the desired closed-loop equilibrium point x_{cl}. Given a general nonlinear system, there are three main steps in the control design process: computing a piecewise-affine (PWA) approximation of the dynamics, designing a PWA controller for this set of dynamics, and proving that this controller stabilizes the original nonlinear plant. The last step can be done using standard robustness methods, such as differential inclusions (see [Boyd *et al.*, 1994] and [Johansson, 1999]) and is not discussed

in this paper. The basic assumption in this paper is that the dynamics of the plant are piecewise-affine, so only the second step in figure 2 will be analyzed. An algorithm for computing a piecewise-affine approximation of a class of nonlinear dynamics is presented in [Rodrigues and How, 2001]. The following sections formulate the synthesis of both state and output feedback PWA controllers for a given PWA system as an optimization problem.

[Figure 2 about here.]

3.1 State Feedback

Following prior analysis of PWA systems [Johansson and Rantzer, 1998a, Pettersson, 1999, Hassibi and Boyd, 1998], consider the piecewise-quadratic Lyapunov function

$$V(x) = \sum_{i=1}^{M} \beta_i(x) V_i(x), \quad V(x) > 0, \quad V \text{ is continuous},$$
$$V_i(x) = \left(x^T P_i x + 2 q_i^T x + r_i \right), \tag{4}$$

where $P_i = P_i^T \in I\!R^{(n \times n)}$, $q_i \in I\!R^n$, $r_i \in I\!R$ and

$$\beta_i(x) = \begin{cases} 1, & x \in \mathcal{R}_i \\ 0, & \text{otherwise} \end{cases}, \tag{5}$$

for $i = 1, \ldots, M$. The expression for the candidate Lyapunov function in each region can be recast as [Johansson and Rantzer, 1998a]

$$V_i(x) = \begin{bmatrix} x \\ 1 \end{bmatrix}^T \begin{bmatrix} P_i & q_i \\ q_i^T & r_i \end{bmatrix} \begin{bmatrix} x \\ 1 \end{bmatrix} = \overline{x}^T \, \overline{P_i} \, \overline{x}. \tag{6}$$

Let α_i be the desired decay rate for this Lyapunov function in each region $\mathcal{R}_i$. Then, defining a performance criterion as

$$\mathcal{J} = \min_{i=1 \ldots M} \alpha_i, \tag{7}$$

the state feedback control design problem is to find from the class of control signals parameterized in the form $u = K_i x + m_i$ in each region $\mathcal{R}_i$, the one that maximizes the performance $\mathcal{J}$. The closed-loop state equations in each region $\mathcal{R}_i$ are

$$\dot{x} = (A_i + B_i K_i)\, x + (b_i + B_i m_i) \equiv \bar{A}_i x + \bar{b}_i. \tag{8}$$

The matrix $\bar{A}_i$ will be designed to be invertible and, therefore, each polytopic region will have a single equilibrium point. Setting x_{cl}^i to be the closed-loop equilibrium point for region $\mathcal{R}_i$ yields the constraint

$$(A_i + B_i K_i)\, x_{cl}^i + (b_i + B_i m_i) = 0. \tag{9}$$

Note that the discussion at the end of this section provides further insight on the selection of x_{cl}^i. Using the boundary description (3), continuity of the candidate Lyapunov function across the boundaries is enforced for each region $\mathcal{R}_i$ and for $j \in \mathcal{N}_i$ by [Hassibi and Boyd, 1998]

$$\begin{aligned} F_{ij}^T(P_i - P_j)F_{ij} &= 0, \\ F_{ij}^T(P_i - P_j)l_{ij} + F_{ij}^T(q_i - q_j) &= 0, \\ l_{ij}^T(P_i - P_j)l_{ij} + 2(q_i - q_j)^T l_{ij} + (r_i - r_j) &= 0. \end{aligned} \tag{10}$$

Remark 2 Note that because $V(x) > 0$ (defined in $\mathbb{R}^n$) is continuous, the fact that V is piecewise-quadratic also implies that V is radially unbounded, *i.e.,* $V(x) \to +\infty$ as $\|x\| \to \infty$, provided $P_i > 0$, $i = 1, \ldots, M$. □

The function $V(x)$ in (4) will be a Lyapunov function with a decay rate of α_i for region $\mathcal{R}_i$ if, for fixed $\epsilon \geq 0$,

$$x \in \mathcal{R}_i \Rightarrow \begin{cases} V_i(x) > \epsilon \|x - x_{cl}\|_2, \\ \dfrac{d}{dt} V_i(x) < -\alpha_i V_i(x). \end{cases} \tag{11}$$

where x_{cl} is the desired closed-loop equilibrium point of the system.

Using the polytopic description of the cells (1) and the $\mathcal{S}-$procedure [Boyd *et al.*, 1994], it can be shown that sufficient conditions for stability with a guaranteed decay rate of α_i for each region $\mathcal{R}_i$ are the existence of $P_i = P_i^T > 0$, q_i, r_i, and matrices Z_i and Λ_i with nonnegative entries satisfying

$$\begin{bmatrix} P_i - \epsilon I_n - \bar{H}_i^T Z_i \bar{H}_i & q_i + \epsilon x_{cl} + \bar{H}_i^T Z_i \bar{g}_i \\ \left(q_i + \epsilon x_{cl} + \bar{H}_i^T Z_i \bar{g}_i\right)^T & r_i - \epsilon x_{cl}^T x_{cl} - \bar{g}_i^T Z_i \bar{g}_i \end{bmatrix} > 0, \tag{12}$$

$$\begin{bmatrix} \bar{A}_i^T P_i + P_i \bar{A}_i + \bar{H}_i^T \Lambda_i \bar{H}_i + \alpha_i P_i & (\cdot) \\ \left(P_i \bar{b}_i + \bar{A}_i^T q_i - \bar{H}_i^T \Lambda_i \bar{g}_i + \alpha_i q_i\right)^T & 2\bar{b}_i^T q_i + \bar{g}_i^T \Lambda_i \bar{g}_i + \alpha_i r_i \end{bmatrix} < 0. \tag{13}$$

where $\bar{H}_i = [0 \;\; h_{i1} \;\; h_{i2} \ldots h_{ip_i}]^T$, $\bar{g}_i = [1 \;\; g_{i1} \;\; g_{i2} \ldots g_{ip_i}]^T$, and I_n is the identity matrix of dimension n.

Remark 3 [Hassibi and Boyd, 1998] It must be ensured that the equilibrium points for the dynamics in each region are the extrema of the corresponding sector of any candidate piecewise-quadratic Lyapunov function. Therefore, if $x_{cl}^i \in \mathcal{R}_i$ is the equilibrium point of region $\mathcal{R}_i$, the constraint $q_i = -P_i x_{cl}^i$ must be included in the optimization. This can be done by writing the Lyapunov function for $\mathcal{R}_i$ as

$$V_i(x) = (x - x_{cl}^i)^T P_i (x - x_{cl}^i) + r_i,$$

and replacing $q_i \to -P_i x_{cl}^i$ and $r_i \to r_i + {x_{cl}^i}^T P_i x_{cl}^i$ in (10), (12) and (13). □

Note that conditions (12) and (13) are only concerned with the behavior of the system in the interior of the polytopic regions, where the derivative of the Lyapunov function along the trajectories of the system is well defined. To guarantee convergence of the trajectories to the closed-loop equilibrium point, it must also be ensured that the trajectories do not stay at a switching boundary for any time interval with positive length, according to the definition 2.1. Equivalently, additional constraints are required on the optimization to ensure that sliding modes [Utkin, 1992] are not generated at the boundaries between polytopic regions. One approach to accomplish this objective is to constrain the component of the vector field $\dot{x}$ perpendicular to the boundaries to be continuous. Defining the sliding surface between regions $\mathcal{R}_i$ and $\mathcal{R}_j$ as $\{x \in I\!R^n \,|\, \sigma_{ij} \equiv c_{ij}^T x - d_{ij} = 0\}$, then $\dot{\sigma}_{ij}$ must be continuous at the boundary with parametric description (3), which yields for each region $\mathcal{R}_i$ the constraint

$$c_{ij}^T \left[(A_i + B_i K_i)(F_{ij} s + l_{ij}) + b_i + B_i m_i \right] = c_{ij}^T \left[(A_j + B_j K_j)(F_{ij} s + l_{ij}) + b_j + B_j m_j \right], \quad (14)$$

$\forall s \in I\!R^{n-1}$, $j \in \mathcal{N}_i$. This equation can be rewritten as

$$\begin{aligned} c_{ij}^T (A_i + B_i K_i - A_j - B_j K_j) F_{ij} &= 0, \\ c_{ij}^T \left[(A_i + B_i K_i - A_j - B_j K_j) l_{ij} + b_i + B_i m_i - b_j - B_j m_j \right] &= 0, \end{aligned} \quad (15)$$

for $i = 1, \ldots, M$ and $j \in \mathcal{N}_i$.

The state feedback synthesis optimization problem is given in the following definition.

Definition 3.1 *The state feedback synthesis optimization problem is*

$$\begin{aligned} \max \quad & \min_i \alpha_i \\ s.t. \quad & (9), \quad (10), \quad (12), \quad (13), \quad (15) \\ & Z_i \succ 0, \; \Lambda_i \succ 0, \; \alpha_i > l_0 \geq 0, \\ & -l_1 \prec K_i \prec l_1, \; -l_2 \prec m_i \prec l_2, \; i = 1, \ldots, M, \end{aligned}$$

where $\succ, \prec$ *mean component-wise inequalities,* l_0 *is a scalar bound and* l_1, l_2 *are vector bounds. Note that the optimization variables are* x^i_{cl}*,* K_i*,* m_i*,* α_i*,* P_i*,* q_i*,* r_i*,* Z_i *and* Λ_i*.* □

This optimization problem is not convex because there are terms involving products of unknowns (such as P_i and B_iK_i and P_i and x^i_{cl} in the constraint $q_i = -P_ix^i_{cl}$). To simplify the optimization problem, the desired closed-loop equilibrium points for each polytopic region, x^i_{cl}, are selected *a-priori* using the optimization algorithm described in [Rodrigues and How, 2001], which makes the constraint $q_i = -P_ix^i_{cl}$ linear in the optimization parameters. Then the products of unknowns appearing in (13) will involve only two variables and this expression is called a *bilinear matrix inequality* (BMI) [Goh *et al.*, 1994]. Algorithms for obtaining local solutions to this BMI optimization problem are presented in Section 3.3.

Remark 4 Continuity of the control signals at the boundaries with parametric description (3) can also be enforced in the optimization, yielding, for each region $\mathcal{R}_i$, the constraints

$$\begin{aligned} (K_i - K_j)F_{ij} &= 0, \\ (K_i - K_j)l_{ij} + (m_i - m_j) &= 0, \forall_j \in \mathcal{N}_i. \end{aligned} \tag{16}$$

Note that (16) imply (15) when $B_i = B_j$ and the plant dynamics are continuous perpendicular to the hyperplane boundaries, so that

$$\begin{aligned} c_{ij}^T (A_i - A_j) F_{ij} &= 0, \\ c_{ij}^T [(A_i - A_j) l_{ij} + b_i - b_j] &= 0, \end{aligned} \tag{17}$$

for $i = 1, \ldots, M$ and $j \in \mathcal{N}_i$. □

Theorem 3.1 *Assume the Lyapunov function (4) is defined in* $\mathcal{X} \subseteq \mathbb{R}^n$*. If there is a solution to the design problem from definition 3.1, the closed-loop system is locally asymptotically stable inside any subset of the largest level set of the control Lyapunov function (4) that is contained in* $\mathcal{X}$*. If* $\epsilon > 0$ *then the convergence is exponential. If, furthermore,* $\mathcal{X} = \mathbb{R}^n$ *then the exponential stability is global.*

Proof: Note that the solution of the optimization problem from definition 3.1 guarantees that sliding modes can not occur at the boundaries between the regions that form the partition. Therefore, the stability analysis in the proof can and will be restricted to the interior of the polytopic regions where the expressions for the Lyapunov function are valid.

We start by noting that the region inside any level set of a Lyapunov function is an invariant set for the system. Since the derivative of the Lyapunov function (well defined in the interior of the polytopic regions) is made strictly negative in the optimization problem in definition 3.1, the invariant sets of the system are also regions of attraction. Thus if $\epsilon > 0$ then $\|x(t) - x_{cl}\|_2 \leq \epsilon^{-1} V(0) e^{-\gamma t}$, where $\gamma = \min_i \alpha_i$, which proves local exponential convergence when $\mathcal{X} \subset I\!R^n$. If, furthermore $\mathcal{X} = I\!R^n$ then the exponential stability is global because, as mentioned in Remark 2, the Lyapunov function (4) is radially unbounded. □

Given this synthesis tool, the next section discusses how it can be extended to address the design of dynamic output feedback controllers.

3.2 Dynamic Output Feedback

The goal of this section is to present the nth order dynamic output feedback controller synthesis problem. It is assumed that the controller has state space representation in each region $\mathcal{R}_j$

$$\begin{array}{rcl} \dot{x}_c & = & A_{c_j} x_c + L_j y + b_{c_j}, \\ u & = & K_j x_c + m_j. \end{array} \tag{18}$$

Using the augmented state $\tilde{x} = [x^T \;\; x_c^T]^T$ and assuming the general case of the plant state being in region $\mathcal{R}_i$ and the controller state in region $\mathcal{R}_j$, the closed-loop dynamics can be rewritten as

$$\dot{\tilde{x}} = \tilde{A}_{ij} \tilde{x} + \tilde{b}_{ij}, \tag{19}$$

$$\tilde{A}_{ij} = \begin{bmatrix} A_i & B_i K_j \\ L_j C_i & A_{c_j} \end{bmatrix}, \quad \tilde{b}_{ij} = \begin{bmatrix} b_i + B_i m_j \\ b_{c_j} \end{bmatrix}.$$

The control Lyapunov function is now

$$V(\tilde{x}) = \sum_{i,j=1}^{M} \beta_{ij}(\tilde{x}) \left(\tilde{x}^T \tilde{P}_{ij} \tilde{x} + 2 \tilde{q}_{ij}^T \tilde{x} + \tilde{r}_{ij} \right), \tag{20}$$

where $\tilde{P}_{ij} = \tilde{P}_{ij}^T \in I\!R^{(2n \times 2n)}$, $\tilde{q}_{ij} \in I\!R^{2n}$, $\tilde{r}_{ij} \in I\!R$ and

$$\beta_{ij}(\tilde{x}) = \begin{cases} 1, & x \in \mathcal{R}_i,\, x_c \in \mathcal{R}_j \\ 0, & \text{otherwise} \end{cases}, \tag{21}$$

for $i, j = 1, \ldots, M$. To derive the continuity conditions for the Lyapunov function note that the facet hyperplane boundaries now belong to one of two classes: boundaries indicating a

plant switch or boundaries indicating a controller switch, described respectively by

$$\tilde{F}_{ij}^{p} = \begin{bmatrix} F_{ij} & 0 \\ 0 & I \end{bmatrix}, \quad \tilde{l}_{ij}^{p} = \begin{bmatrix} l_{ij} \\ 0 \end{bmatrix},$$

$$\tilde{F}_{ij}^{c} = \begin{bmatrix} I & 0 \\ 0 & F_{ij} \end{bmatrix}, \quad \tilde{l}_{ij}^{c} = \begin{bmatrix} 0 \\ l_{ij} \end{bmatrix}.$$

To renumber the cells using only one index, for a given i and j we associate an index $k = T(i,j)$, where T is an injective mapping. Using this notation, the continuity conditions (10) can be rewritten as

$$\begin{aligned} \tilde{F}_{kh}^{T}(\tilde{P}_k - \tilde{P}_h)\tilde{F}_{kh} &= 0, \\ \tilde{F}_{kh}^{T}(\tilde{P}_k - \tilde{P}_h)\tilde{l}_{kh} + \tilde{F}_{kh}^{T}(\tilde{q}_k - \tilde{q}_h) &= 0, \\ \tilde{l}_{kh}^{T}(\tilde{P}_k - \tilde{P}_h)\tilde{l}_{kh} + 2(\tilde{q}_k - \tilde{q}_h)^{T}\tilde{l}_{kh} + \tilde{r}_k - \tilde{r}_h &= 0, \end{aligned} \tag{22}$$

for $k = 1, \ldots, M^2$ and $h \in \mathcal{N}_k$. The next step is to derive the constraints to avoid sliding modes at the boundaries. Because of the structure of the augmented state space, there are three possible switching scenarios:

1. The state of the plant switches at a plant hyperplane boundary,
2. The state of the controller switches at a controller hyperplane boundary,
3. Both of the above switches occur at the same time.

Cases 1 and 2 can cause sliding modes at a hyperplane boundary of dimension $2n-1$, while case 3 can cause sliding modes at a $2n-2$ dimensional hyperplane.

Case 1: Assume that the controller state remains in $\mathcal{R}_k$ while the plant switches from $\mathcal{R}_i$ to $\mathcal{R}_j$. Following the derivation presented in Section 3.1 in Eq. (15), with $c^T = [c_{ij}^T \, 0^T]$, yields

$$\begin{aligned} c_{ij}^{T}\left(A_i - A_j\right) F_{ij} &= 0, \\ c_{ij}^{T}\left(B_i - B_j\right) K_k &= 0, \\ c_{ij}^{T}\left[\left(A_i - A_j\right) l_{ij} + b_i - b_j + \left(B_i - B_j\right) m_k\right] &= 0, \end{aligned} \tag{23}$$

for $i, k = 1, \ldots, M,\ j \in \mathcal{N}_i$. Note that the first constraint is only on the plant parameters. One important set of piecewise-affine dynamics that verify this constraint are PWA models that are continuous perpendicular to the hyperplane boundaries between polytopic regions,

as described in (17). However, the class of systems that verify the first constraint in (23) is broader because the second constraint in (17) does not need to be satisfied in (23).

Case 2: Assume that the plant state remains in $\mathcal{R}_i$ while the controller switches from $\mathcal{R}_k$ to $\mathcal{R}_h$. Following the derivation in Section 3.1, with $c^T = [0^T \; c_{kh}^T]$, yields the constraints

$$\begin{aligned} c_{kh}^T \left(L_k - L_h\right) C_i &= 0, \\ c_{kh}^T \left(A_{c_k} - A_{c_h}\right) F_{kh} &= 0, \\ c_{kh}^T \left[\left(A_{c_k} - A_{c_h}\right) l_{kh} + b_{c_k} - b_{c_h}\right] &= 0, \end{aligned} \tag{24}$$

for $i, k = 1, \ldots, M$ and $h \in \mathcal{N}_k$.

Case 3: Following the same reasoning, when both states switch at the same time, the constraints are

$$\begin{aligned} c_{ij}^T \left(A_i - A_j\right) F_{ij} &= 0, \\ c_{ij}^T \left(B_i K_k - B_j K_h\right) F_{kh} &= 0, \\ c_{ij}^T \left[\left(A_i - A_j\right) l_{ij} + \left(B_i K_k - B_j K_h\right) l_{kh} + b_i - b_j + B_i m_k - B_j m_h\right] &= 0, \\ c_{kh}^T \left(L_k C_i - L_h C_j\right) F_{ij} &= 0, \\ c_{kh}^T \left(A_{c_k} - A_{c_h}\right) F_{kh} &= 0, \\ c_{kh}^T [\left(A_{c_k} - A_{c_h}\right) l_{kh} + \left(L_k C_i - L_h C_j\right) l_{ij} + b_{c_k} - b_{c_h}] &= 0, \end{aligned} \tag{25}$$

for $i, k = 1, \ldots M$, $j \in \mathcal{N}_i$ and $h \in \mathcal{N}_k$. Therefore, the combined set of sliding modes constraints are given by Eqs. (23)–(25). These constraints guarantee that the component of the vector field $\dot{\tilde{x}}$ perpendicular to the sliding surfaces of the plant ($\sigma_{ij}^p \equiv c_{ij}^T x - d_{ij} = 0$) and the controller ($\sigma_{kh}^c \equiv c_{kh}^T x_c - d_{kh} = 0$) will be continuous.

Similar to the state feedback case, there is still the equilibrium point equality constraint to be added to the design. Denoting the closed-loop equilibrium point of each region $\mathcal{R}_k \equiv \mathcal{R}_i \times \mathcal{R}_j$, $k = T(i,j)$ by $\tilde{x}_{cl}^k, k = 1, \ldots, M^2$ yields the constraint

$$\tilde{A}_k \tilde{x}_{cl}^k + \tilde{b}_k = 0. \tag{26}$$

Because of the dynamic output feedback structure, the parameters in (12)–(13) must be modified, with $\bar{A}_i \to \tilde{A}_k$, $\bar{b}_i \to \tilde{b}_k$, $P_i \to \tilde{P}_k$, $q_i \to \tilde{q}_k$ and $r_i \to \tilde{r}_k$, which yields

$$\begin{bmatrix} \tilde{P}_k - \epsilon I_{2n} - \bar{H}_k^T Z_k \bar{H}_k & \tilde{q}_k + \epsilon \tilde{x}_{cl} + \bar{H}_k^T Z_k \bar{g}_k \\ \left(\tilde{q}_k + \epsilon \tilde{x}_{cl} + \bar{H}_k^T Z_k \bar{g}_k\right)^T & \tilde{r}_k - \epsilon \tilde{x}_{cl}^T \tilde{x}_{cl} - \bar{g}_k^T Z_k \bar{g}_k \end{bmatrix} \; > \; 0, \tag{27}$$

$$\begin{bmatrix} \tilde{A}_k^T\tilde{P}_k + \tilde{P}_k\tilde{A}_k + \bar{H}_k^T\Lambda_k\bar{H}_k + \alpha_k\tilde{P}_k & \left(\tilde{P}_k\tilde{b}_k + \tilde{A}_k^T\tilde{q}_k - \bar{H}_k^T\Lambda_k\bar{g}_k + \alpha_k\tilde{q}_k\right) \\ \left(\tilde{P}_k\tilde{b}_k + \tilde{A}_k^T\tilde{q}_k - \bar{H}_k^T\Lambda_k\bar{g}_k + \alpha_k\tilde{q}_k\right)^T & 2\tilde{b}_k^T\tilde{q}_k + \bar{g}_k^T\Lambda_k\bar{g}_k + \alpha_k\tilde{r}_k \end{bmatrix} < 0. \qquad (28)$$

where $\epsilon \geq 0$ is fixed, $\tilde{H}_k = [H_k^T\, 0]^T$, $\bar{H}_k$, $\bar{g}_k$ are defined as before with $H_k \to \tilde{H}_k$, and $\tilde{x}_{cl}$ is the desired closed-loop equilibrium point for the system. The terms $\tilde{q}_k$ and $\tilde{r}_k$ should be further modified according to Remark 3. As before, with $\tilde{x}_{cl}^i$ selected *a-priori*, inequality (28) is a BMI. The optimization problem is given in the following definition.

Definition 3.2 *The dynamic output feedback synthesis optimization problem is*

$$\begin{aligned} \max \quad & \min_i \alpha_i \\ s.t. \quad & (22),\ (23),\ (24),\ (25),\ (26),\ (27),\ (28) \\ & Z_i \succ 0,\ \Lambda_i \succ 0,\ \alpha_i > l_0 \geq 0, \\ & -l_1 \prec K_i \prec l_1,\ -l_2 \prec m_i \prec l_2,\ -l_3 \prec L_i \prec l_3,\ i = 1, \ldots, M^2, \end{aligned}$$

where $\succ$, $\prec$ *mean component-wise inequalities,* l_0 *is a scalar bound and* l_1, l_2, l_3 *are vector bounds.* □

Algorithms for solving this problem for a suboptimal solution are presented in Section 3.3.

Remark 5 Conditions (16) can still be used to enforce continuity of the control signals at the boundaries, with matrices F_{ij} and l_{ij} describing the hyperplane boundary indicating a controller switch. Another way to enforce continuity of the control is to include what are effectively actuator dynamics into the plant. For example, with $x_c \in \mathcal{R}_j$, assume that the actuator dynamics are m decoupled first-order systems

$$\begin{aligned} u_c &= K_j x_c + m_j, \qquad (29) \\ \dot{u} &= -\tau_j u + \tau_j u_c, \end{aligned}$$

where u_c is the (potentially discontinuous) output of the controller that is smoothed by the filter dynamics into the actual plant input signal u. The order of the system dynamics will then increase by m states. Note that the diagonal matrix τ_j can be optimized as part of the control design. □

Remark 6 To be able to switch based on state estimates rather than measured outputs, a controller with the structure of a regulator and an observer must be designed. For the plant dynamics (2), the state estimate $\hat{x}$ can be obtained using a Luenberger structure for

the regulator/observer in each region $\mathcal{R}_i$ with description

$$\dot{\hat{x}} = A_i\hat{x} + B_iu + b_i + L_i\left(y - C_i\hat{x}\right) \quad (30)$$

$$u = K_i\left(\hat{x} - x_{cl}^i\right) + m_i \quad (31)$$

Using the plant dynamics (2) and the controller dynamics (30), it can be shown that the closed-loop system can still be described by (19) using the augmented state $\tilde{x} = [x^T \;\; x_c^T]^T$ with $x_c = \hat{x} - x_{cl}^i$ for each region $\mathcal{R}_i$. The additional constraints

$$A_{c_i} = A_i + B_iK_i - L_iC_i, \quad (32)$$

$$b_{c_i} = B_im_i + b_i + \left(A_i - L_iC_i\right)x_{cl}^i \quad (33)$$

must also be enforced. Solving the regulator/observer synthesis problem extends the results in Ref. [Boyd *et al.*, 1994] to the case of piecewise-affine systems.

Note that the state estimation controller structure has the property that zero estimation error is an invariant of the closed-loop system. In other words, if $x(0) = \hat{x}(0)$ then both the plant state and the controller state start in the same region. Moreover, defining $\delta x(t) = x(t) - \hat{x}(t)$, using (19) and (30) with $i = j$ and $x_c = \hat{x} - x_{cl}^i$, the dynamics of $\delta x(t)$ can be written as $\dot{\delta x}(t) = \left(A_i - L_iC_i\right)\delta x(t)$. Thus if $\delta x(0) = 0$, then $\delta x(t) = 0$, $\forall t > 0$. □

Corollary 3.1 *Assume the Lyapunov function (20) is defined in $\mathcal{X} \subseteq \mathbb{R}^{2n}$. If there is a solution to the design problem from definition 3.2, then the closed-loop system is locally asymptotically stable inside any subset of the largest level set of the control Lyapunov function (20) that is contained in $\mathcal{X}$. If $\epsilon > 0$ then the convergence is exponential. If, furthermore $\mathcal{X} = \mathbb{R}^{2n}$ then the exponential stability is global.*

Proof: Similar to the proof of Theorem 3.1 replacing x by $\tilde{x}$, x_{cl} by $\tilde{x}_{cl}$ and the state space $\mathbb{R}^n$ by $\mathbb{R}^{2n}$. □

3.3 Local Solution Algorithms

This section investigates the use of two algorithms from the existing literature to solve the bi-convex optimization problems for a suboptimal solution. The two algorithms are the alternating method [Goh *et al.*, 1994] (or V–K iteration [Banjerdpongchai and How, 2000, Paré *et al.*, 2001]) and the *Path-Following* Method [Hassibi *et al.*, 1999b]. It is also shown how these can be combined into a hybrid method. Note that, while branch and bound

algorithms are available for solving $\mathcal{NP}$-hard BMI optimization problems for the optimal solution [Goh *et al.*, 1994], these algorithms run in non-polynomial time because they consist of global searches. Therefore, they are typically not computationally tractable for designing dynamic controllers using a medium/large number of polytopic regions. Although suboptimal, local algorithms consist of an iterative scheme that, at each iteration, executes efficient polynomial-time algorithms and thus can provide (suboptimal) solutions in a reasonable amount of computational time. The following discusses three local solution methods and applies them to the dynamic output feedback optimization problem. The first method is the V–K iteration.

Algorithm # 1 – The V–K iteration: The basic idea of the V–K iteration is that a BMI can be converted into a LMI when some of the parameters in the BMI are fixed to be constant. One algorithm for solving an optimization problem with BMI constraints is to alternate between two optimization problems subject to LMIs, with each problem corresponding to fixing one of the two parameters involved in the BMI. This method has been called the alternating method or V–K iteration because the parameters that are fixed and then solved for in the alternating steps are typically the Lyapunov function V and the controller K. The algorithm is suboptimal because the search for the optimal parameters is done only in restricted directions. To solve the optimization problem in definition 3.2 for a suboptimal solution, the V–K iteration consists of:

***V*-Step**: Given a fixed controller and fixed α_i, solve

$$\begin{array}{ll} \text{find} & \tilde{P}_i,\ \tilde{r}_i, \\ s.t. & (22),\quad (27),\quad (28) \\ & Z_i \succ 0,\ \Lambda_i \succ 0, \qquad i = 1, \ldots, M^2 \end{array}$$

***K*-Step**: Fix the parameters $\tilde{P}_i,\ \tilde{r}_i$ and solve

$$\begin{array}{ll} \max & \min\limits_i \alpha_i \\ s.t. & (23),\ (24),\ (25),\ (26),\ (27),\ (28) \\ & Z_i \succ 0,\ \Lambda_i \succ 0,\ \alpha_i > l_0 \geq 0, \\ & -l_1 \prec K_i \prec l_1,\ -l_2 \prec m_i \prec l_2,\ -l_3 \prec L_i \prec l_3,\ i = 1, \ldots, M^2, \end{array}$$

where, as before, $\succ$, $\prec$ mean component-wise inequalities, l_0 is a scalar bound and $l_1,\ l_2,\ l_3$ are vector bounds. This iterative loop is repeatedly executed until there is no major improvement in the cost relative to the previous iteration, or until the LMIs are reported to be infeasible.

Remark 7 Using slack variables, the K-Step can be rewritten with a linear objective and

therefore it can be formulated as a semi-definite program, which is a convex optimization program that can be solved efficiently using available software. □

Remark 8 The fixed α_i, $i = 1, \ldots M^2$, in the V-Step should be the ones obtained in the K-Step of the previous iteration. Constraining α_i to be upper bounded (by a large number) and adding the constraint that the performance index should be higher than the one obtained in the previous iteration guarantees the convergence of the V–K iteration. In particular, convergence follows from the fact that the sequence of performance indices is monotonically increasing and upper bounded. □

Remark 9 Constraints (32) and (33) should be added to the K-step to obtain a regulator/observer structure. □

Algorithm # 2 – Path-Following: The path-following/homotopy method performs a first order approximation by linearizing the BMI. The resulting optimization problem can then be solved to obtain a perturbation to the current solution that improves the performance criterion. This linearization process can then be repeated to compute successive small perturbations to the optimization parameters that incrementally improve the performance objective and can ultimately lead to a large improvement in performance. Note that the updates to the parameters should be constrained to be small so that the linearization approximations are valid. This same approach was used to solve several BMI problems in [Hassibi *et al.*, 1999b].

This process is an approximation to continually changing the performance along a path to the (suboptimal) solution, which is the reason why it has been called a path-following (or homotopy) method. The advantage of this method relative to the V–K iteration is that the optimization simultaneously searches for perturbations to both the Lyapunov function and the controller parameters. The disadvantage is that smaller steps are being performed during each iteration. Thus it might be necessary to run many more iterations than would be required with the V–K iteration to obtain similar improvements in the performance.

At each iteration, the new perturbations are the quantities that are optimized while the nominal values are the ones resulting from the previous iteration. More precisely, let

$$\begin{array}{lll} \tilde{P}_i = \tilde{P}_i^0 + \delta\tilde{P}_i, & \tilde{q}_i = \tilde{q}_i^0 + \delta q_i, & \tilde{r}_i = \tilde{r}_i^0 + \delta\tilde{r}_i, \\ K_i = K_i^0 + \delta K_i, & L_i = L_i^0 + \delta L_i, & m_i = m_i^0 + \delta m_i \\ A_{c_i} = A_{c_i}^0 + \delta A_{c_i}, & b_{c_i} = b_{c_i}^0 + \delta b_{c_i}, & \alpha_i = \alpha_i^0 + \delta\alpha_i. \end{array}$$

The matrix $\tilde{A}_{ij}$ and the vector $\tilde{b}_{ij}$ from (19) will also have nominal parts $\tilde{A}^0_{ij}$, $\tilde{b}^0_{ij}$ and perturbations $\delta\tilde{A}_{ij}$, $\delta\tilde{b}_{ij}$, respectively, which are defined accordingly. Defining now

$$\begin{aligned} a &= \tilde{A}_i^T\tilde{P}_i^0 + \tilde{P}_i^0\tilde{A}_i + \tilde{A}_i^{0^T}\delta\tilde{P}_i + \delta\tilde{P}_i\tilde{A}_i^0, \\ b &= \alpha_i\tilde{P}_i^0 + \alpha_i^0\delta\tilde{P}_i, \qquad c = \tilde{P}_i^0\tilde{b}_i + \delta\tilde{P}_i\tilde{b}_i^0, \qquad d = \tilde{A}_i^T\tilde{q}_i^0 + (\tilde{A}_i^0)^T\delta q_i, \\ e &= \alpha_i\tilde{q}_i^0 + \alpha_i^0\delta\tilde{q}_i, \qquad f = \tilde{b}_i^T\tilde{q}_i^0 + (\tilde{b}_i^0)^T\delta\tilde{q}_i, \qquad g = \alpha_i\tilde{r}_i^0 + \alpha_i^0\delta\tilde{r}_i, \end{aligned}$$

the first order approximation of the BMI (28) is

$$\begin{bmatrix} a + \bar{H}_i^T\Lambda_i\bar{H}_i + b & \Big(c + d - \bar{H}_i^T\Lambda_i\bar{g}_i + e\Big) \\ \Big(c + d - \bar{H}_i^T\Lambda_i\bar{g}_i + e\Big)^T & 2f + \bar{g}_i^T\Lambda_i\bar{g}_i + g \end{bmatrix} < 0. \tag{34}$$

The path-following method is then described as

Path-Following Step: Solve

$$\begin{aligned} \max \quad & \min_i \alpha_i \\ s.t. \quad & (22),\ (23),\ (24),\ (25),\ (26),\ (27),\ (34) \\ & Z_i \succ 0,\ \Lambda_i \succ 0,\ \alpha_i > l_0 \geq 0, \\ & -l_1 \prec K_i \prec l_1,\ -l_2 \prec m_i \prec l_2,\ -l_3 \prec L_i \prec l_3,\ i = 1, \ldots, M^2, \end{aligned}$$

where $\succ$, $\prec$ are defined as before. The absolute value of all perturbations should also be constrained to be a fraction of the absolute value of the corresponding nominal parameters so that the first order approximation of the BMI is valid. Also, as before, this iterative loop is repeatedly executed until there is no major improvement in the cost relative to the previous iteration, or until the LMIs are reported to be infeasible.

Algorithm # 3 – Hybrid Method: The two previous algorithms can be combined by changing the K-step of the V–K iteration to perform a combined search of the perturbations to the Lyapunov function and the controller parameters. Once a controller is obtained from this process, the V-step is then changed so that it searches for an optimal Lyapunov function for that controller by minimizing the maximum condition number of the $\tilde{P}_i$ matrices. Notice that this is stronger than simply searching for a feasible Lyapunov function and should therefore yield better results than simply using the Lyapunov function obtained from the original path-following method. The hybrid algorithm is then defined as follows:

***V*-Step**: Given a fixed controller and fixed α_i, solve

$$\begin{array}{ll} \min & \max_i \operatorname{cond}\left(\tilde{P}_i\right) \\ s.t. & (22),\quad (27),\quad (28) \\ & Z_i \succ 0,\ \Lambda_i \succ 0, \qquad i = 1, \ldots, M^2 \end{array}$$

***K*-Step**: Same as Path-Following step.

Remark 10 Again, using slack variables, the V-Step can be rewritten with a linear objective and therefore it can also be formulated as a semi-definite program. □

Remark 11 These iteration algorithms can be initialized with a controller designed using a patched LQG. In fact, it was shown in [Rodrigues *et al.*, 2000] that an LQG controller can be designed for each region $\mathcal{R}_i$ to yield the controller parameters K_i, L_i and A_{c_i}. The parameter m_i is obtained from the solution of the equation $A_i x_{cl}^i + b_i + B_i m_i = 0$ and the parameter b_{c_i} is then $b_{c_i} = -L_i C_i x_{cl}^i$. □

Note that for medium/large scale problems it might be difficult to develop good initial conditions for the full optimization problem in definition 3.2. This difficulty is associated with the additional complexity of the output feedback problem generated by the augmented state space structure and the corresponding partition. A useful and effective heuristic in those cases is to divide the output feedback synthesis into two steps:

1. Nominal design, which assumes that the controller and plant states start in the same region and always switch at the same time,
2. Extended design, which assumes that the nominal controller is used to initialize an iteration process designed to increase the region of stability.

The following sections describe each of these steps in detail.

3.3.1 Nominal Design

The results in this section assume that the controller and plant state start in the same region and always switch at the same time so that $i = j$ in (19). For notational simplicity, the subscript ii will be replaced by just i. This assumption simplifies the sliding mode constraints, which reduce to

$$c_{ij}^T \left(A_i + B_i K_i - A_j - B_j K_j\right) F_{ij} \;=\; 0,$$

$$
\begin{aligned}
c_{ij}^T \left((A_i + B_i K_i - A_j - B_j K_j)\, l_{ij} + b_i - b_j + B_i m_i - B_j m_j \right) &= 0, \\
c_{ij}^T \left(A_{c_i} - A_{c_j} + L_i C_i - L_j C_j \right) F_{ij} &= 0, \\
c_{ij}^T [\left(A_{c_i} - A_{c_j} + L_i C_i - L_j C_j \right) l_{ij} + b_{c_i} - b_{c_j}] &= 0,
\end{aligned} \tag{35}
$$

for $i = 1, \ldots M$, $j \in \mathcal{N}_i$.

The control optimization problem from definition 3.2 will then be solved only for the "diagonal" regions $\mathcal{R}_i \times \mathcal{R}_i$, $i = 1, \ldots, M$ with the sliding mode constraints (23)-(25) replaced by (35). This greatly simplifies the complexity of the output feedback control design problem.

The assumptions in this section are very stringent. However, they enable the design of a controller using an optimization procedure that grows linearly with the number of polytopic regions for each of the state vectors x and x_c. In fact, given M polytopic regions for each of the state vectors, only M of the M^2 possible combinations are considered in the nominal design process. This simplified control design can then be analyzed to determine if it satisfies the overall constraints and/or used to initialize the extended design process.

3.3.2 Extended Design

The nominal designs in the previous section can be used to initialize a second process that designs controllers for which at least local stability results can be guaranteed under broader classes of switching rules. To reduce computational complexity, the design will be constrained to a subset of the state space called the *design set*.

Definition 3.3 *A design set $\mathcal{D}$ is a nonempty closed subset of the domain of the state variable $\tilde{x} = [x^T \quad x_c^T]^T$, where $x \in \mathbb{R}^n$ is the state of the plant and $x_c \in \mathbb{R}^n$ is the state of the controller.* □

One example is the nearest neighbor design set which corresponds to the region of the state space containing all cells (i, j) with $i = 1, \ldots, M$ and $j \in \mathcal{N}_i$. The design space in Section 3.3.1 was the set corresponding to the region of the state space containing all cells (i, i).

Definition 3.4 *Given a design set $\mathcal{D}$, the extended design iteration consists of the local solution (by any of the algorithms from Section 3.3) of the problem in definition 3.2 modified in the following two ways:*

1. *The number of sectors of the control Lyapunov function (20) are equal to the number of regions $\mathcal{R}_k$, $k = T(i, j)$ such that $\mathcal{R}_k \cap \mathcal{D} \neq \emptyset$,*

2. The initial controller is the one obtained from the nominal design in Section 3.3.1. □

It is possible that the extended design stage merely consists of a post-analysis of the nominal design, provided all sliding modes constraints are included in that design.

Corollary 3.2 *If there is a solution to the extended design iteration from definition 3.4, the closed-loop system is locally asymptotically stable inside any subset of the largest level set of the control Lyapunov function (20) that is contained in $\mathcal{D}$. If $\epsilon > 0$ then the convergence is exponential. If, furthermore $\mathcal{D} = I\!R^{2n}$ then the exponential stability is global.*

Proof: Similar to the proof of Corollary 3.1 with $\mathcal{X}$ replaced by $\mathcal{D}$. □

Remark 12 When using the V–K iteration, the V-step can be changed to solve the problem of finding the Lyapunov function that maximizes the volume of the invariant set verifying the conditions of Corollary 3.2. However, this problem is not convex. □

4 Examples

This section uses the synthesis techniques discussed previously to design controllers for several examples using the semidefinite program package **sdpsol** [Wu and Boyd, 2000]. Except when otherwise discussed, the iterative solution algorithms were initialized using a patched LQR or LQG, as described in Remark 11 [Rodrigues *et al.*, 2000]. For all examples with nonlinear plant dynamics, the algorithm in [Rodrigues and How, 2001] was used to approximate these dynamics with a piecewise-affine model. Although the controllers were designed for this PWA approximation, their performance was simulated using the full nonlinear model. To theoretical guarantee that the controller also stabilizes the original nonlinear system, standard robustness methods, such as differential inclusions (see [Boyd *et al.*, 1994, Johansson, 1999]) and norm bounds on the approximation error [Johansson, 1999], could be used in the controller design. However, this issue was not addressed in this paper. The closed-loop equilibrium points for these examples were selected using the optimization algorithm in [Rodrigues and How, 2001]. In all examples, the Lyapunov function was designed to minimize the maximum condition number of the P_i matrices corresponding to the quadratic terms on the state.

There are a total of four examples. Example 1 shows state feedback controller synthesis for a third-order plant with the closed-loop equilibrium point at the origin. The special feature of this example is that the BMI (13) must be changed for the region containing the

origin because of problems with strict infeasibility. In particular, for the region containing the origin $x^i_{cl} = x_{cl} = 0$, so $q_i = -P_i x^i_{cl} = 0$. Also, the dynamics are linear rather than affine so $b_i = m_i = 0$. Because of these simplifications, the inequalities (12) and (13) are not strictly feasible, but this problem can be resolved by replacing condition (13) for affine dynamics by the standard inequality for linear dynamics, *i.e.,* $A_i^T P_i + P_i A_i + \alpha_i P_i < 0$. [Boyd *et al.*, 1994, Pettersson, 1999] provide a detailed discussion of alternative methods for solving the strict feasibility problem.

Example 2 presents a state feedback design for a fourth-order open-loop unstable system that has multiple equilibrium points and a complex nonlinearity that depends on two variables. A further interesting feature of this example is that the initial controller does not verify the conditions for avoiding sliding modes, but the synthesis procedure yields a controller that satisfies these constraints. Example 3 presents an output feedback controller for a first-order unstable plant. A key objective of this example is to compare two of the iterative algorithms in Section 3.3. Example 4 illustrates a more complex output feedback control problem for a bi-stable circuit with multiple equilibrium points for which the actuator dynamics were included in the design.

Example 1: The objective of this example is to design a controller that forces a cart on the $x - y$ plane to follow the straight line $y = 0$ with a constant velocity $u_0 = 1$ m/s. It is assumed that a controller has already been designed to maintain a constant forward velocity. The cart's path is then controlled by the torque T about the z-axis according to the following dynamics:

$$\begin{bmatrix} \dot{\psi} \\ \dot{r} \\ \dot{y} \end{bmatrix} = \begin{bmatrix} 0 & 1 & 0 \\ 0 & -\frac{k}{I} & 0 \\ 0 & 0 & 0 \end{bmatrix} \begin{bmatrix} \psi \\ r \\ y \end{bmatrix} + \begin{bmatrix} 0 \\ 0 \\ u_0 \sin(\psi) \end{bmatrix} + \begin{bmatrix} 0 \\ \frac{1}{I} \\ 0 \end{bmatrix} T, \tag{36}$$

where ψ is the heading angle with time derivative r, $I = 1$ Kgm^2 is the moment of inertia of the cart with respect to the center of mass, $k = 0.01$ is the damping coefficient, and T is the control torque. The state of the system is $(x_1, x_2, x_3) = (\psi, r, y)$. Assume the trajectories can start from any possible initial angle and any initial distance from the line in the range $y_0 \in [-10, 10]$ m. Note that the closed-loop system will always have equilibrium points at $\psi = \pm\pi$ which cannot be changed by the controller. Therefore, asymptotic stability can only be guaranteed for a strip in the variable y, *i.e.,* for $y \in (y_{\min}, y_{\max})$ for some $y_{\min}$ and $y_{\max}$. Because the objective was to design a controller that stabilizes the system in the largest possible region inside the strip $y_0 \in [-10, 10]$ m, we set $y_{\max} = -y_{\min} = 12$.

A seven sector piecewise-affine approximation of $\sin(\psi)$ was used in the design, with the three regions close to the origin ($\psi \in \left[-\frac{\pi}{5}, \frac{\pi}{5}\right]$) being smaller than the other four. The resulting

polytopic regions are:

$$\begin{aligned}
\mathcal{R}_1 &= \{x \in I\!R^3 \,|\, x_1 \in \left(-\pi, -\frac{3\pi}{5}\right),\, x_3 \in (-12, 12)\},\\
\mathcal{R}_2 &= \{x \in I\!R^3 \,|\, x_1 \in \left(-\frac{3\pi}{5}, -\frac{\pi}{5}\right),\, x_3 \in (-12, 12)\},\\
\mathcal{R}_3 &= \{x \in I\!R^3 \,|\, x_1 \in \left(-\frac{\pi}{5}, -\frac{\pi}{15}\right),\, x_3 \in (-12, 12)\},\\
\mathcal{R}_4 &= \{x \in I\!R^3 \,|\, x_1 \in \left(-\frac{\pi}{15}, \frac{\pi}{15}\right),\, x_3 \in (-12, 12)\},
\end{aligned}$$

and $\mathcal{R}_5$ is symmetric to $\mathcal{R}_3$, $\mathcal{R}_6$ is symmetric to $\mathcal{R}_2$ and $\mathcal{R}_7$ is symmetric to $\mathcal{R}_1$, all with respect to the origin.

[Figure 3 about here.]

An initial state feedback controller was designed for the middle region $\mathcal{R}_4$ using LQR with the weighting matrices

$$Q = \begin{bmatrix} 125 & 0 & 0 \\ 0 & 10 & 0 \\ 0 & 0 & 9 \end{bmatrix}, \quad R = 10.$$

The corresponding matrix gain is

$$K_4 = \begin{bmatrix} -4.2807 & -3.0822 & -0.9487 \end{bmatrix} \text{ and } m_4 = 0.$$

The controller gains for the other regions were designed using the conditions (16) for continuity of the control input (and avoidance of sliding modes, because the matrix B is constant and the approximate plant dynamics are piecewise-affine and continuous). Using a notation where the superscript indicates the state component and the subscript indicates the region, conditions (16) are rewritten as

$$K_i^r = K_j^r, \tag{37}$$

$$K_i^y = K_j^y, \tag{38}$$

$$\psi_{ij}\left(K_i^\psi - K_j^\psi\right) + m_i - m_j = 0, \tag{39}$$

where ψ_{ij} is the value of the heading angle at the boundary between regions $\mathcal{R}_i$ and $\mathcal{R}_j$. The conditions (9) for fixing the location of the equilibrium points are $\psi_{eq} = -b_i/a_i$, $r_{eq} = 0$ and

$$K_i^\psi \psi_{eq} + K_i^y y_{eq} + m_i = 0, \tag{40}$$

where the piecewise-affine approximation of $\sin(\psi)$ is described by $a_i\psi + b_i$ for each region $\mathcal{R}_i$. Selecting the location for the equilibrium points at[1]

$$x_{cl}^1 = \begin{bmatrix} -\pi \\ 0 \\ 12.1162 \end{bmatrix}, \; x_{cl}^2 = \begin{bmatrix} 1.4050 \\ 0 \\ 1.0380 \end{bmatrix}, \; x_{cl}^3 = \begin{bmatrix} 0.0198 \\ 0 \\ -1.6188 \end{bmatrix},$$
$$x_{cl}^4 = 0, \; x_{cl}^5 = -x_{cl}^3, \qquad x_{cl}^6 = -x_{cl}^2, \; x_{cl}^7 = -x_{cl}^1,$$

one can start in region $\mathcal{R}_4$ and recursively solve equations (37)–(40) for K_j and m_j given K_i and m_i with $j = i-1$ and $j = i+1$. Furthermore, given the symmetry of the problem, these equations need only be solved recursively for $j = i-1$, $i = 4, 3, 2$. The remaining controller parameters can be obtained from the symmetry constraints

$$K_5 = K_3, \; K_6 = K_2, \; K_7 = K_1, \quad \text{and} \quad m_5 = -m_3, \; m_6 = -m_2, \; m_7 = -m_1.$$

The V–K iteration algorithm, with parameters $l_0 = 10^{-7}$, $l_1 = 10$, $l_2 = 20$ and $\epsilon = 10^{-4}$, was run using this controller as the initial input. The constraints of controller symmetry and $P_5 = P_3$, $P_6 = P_2$, $P_7 = P_1$, $r_5 = r_3$, $r_6 = r_2$, $r_7 = r_1$ and $\alpha_5 = \alpha_3$, $\alpha_6 = \alpha_2$, $\alpha_7 = \alpha_1$ were added to the design. After four iterations, the resulting controller is parameterized by

$$\begin{aligned} K_1 &= [\; -4.2916 \quad -5.0022 \quad -1.0282 \;], \quad m_1 = -1.0248 \\ K_2 &= [\; -1.8230 \quad -5.0022 \quad -1.0282 \;], \quad m_2 = 3.6284 \\ K_3 &= [\; -9.9335 \quad -5.0022 \quad -1.0282 \;], \quad m_3 = -1.4676 \\ K_4 &= [\; -2.9264 \quad -5.0022 \quad -1.0282 \;], \quad m_4 = 0.0 \end{aligned}$$

The corresponding Lyapunov function is shown in figure 3 as a function of ψ and y with r fixed. The figure shows that the shape of the Lyapunov function is quite complex, which illustrates that the piecewise-quadratic functions form a much broader class than globally quadratic functions.

[Figure 4 about here.]

[Figure 5 about here.]

Using the results of Theorem 3.1, the closed-loop piecewise-affine system is exponentially

[1]Note that only y_{eq} can be selected freely and, for regions $\mathcal{R}_1$ and $\mathcal{R}_7$, y_{eq} should be outside the interval of possible initial conditions.

stable with a guaranteed decay rate of at least $\min_i \alpha_i = 0.0151$ inside the largest level set contained in

$$\mathcal{D} = \{(\psi, r, y) \,|\, \psi \in [-\pi, \pi],\, y \in [-12, 12],\, \forall r\}$$

which will be denoted as $\mathcal{S}$. The projection of $\mathcal{S}$ on the $\psi \times y$ plane is shown in figure 4 by the region inside the outermost closed curve. Note that, as expected, $\mathcal{S} \subset \mathcal{D}$. Note also that the region $\mathcal{S}$ primarily extends in a direction of positive (negative) values of ψ for negative (positive) y values, which is consistent with the direction that the cart would need to be pointed to return to the line $y = 0$ that must be tracked. Figure 4 also shows the response of the nonlinear plant in a feedback connection with the controller along several trajectories starting inside the region of attraction, which are over-plotted with the level curves to show the asymptotic convergence to the origin. Note that the level sets of the Lyapunov function, which are invariant sets for the trajectories of the piecewise-affine approximation, will not necessarily be invariant sets for the nonlinear system trajectories. Figures 5–7 provide a more detailed analysis of these system trajectories for a particular initial condition. The plots clearly show that the closed-loop system tracks the straight line $y = 0$, even when the nonlinear plant dynamics are used. Therefore, the controller performs as desired.

[Figure 6 about here.]

Example 2: Consider the problem of controlling an inverted pendulum (on a cart) to its open-loop unstable equilibrium point. Because the pendulum can start anywhere within ± 45 degrees of vertical, the full nonlinear dynamics must be used. This problem can be addressed by approximating the nonlinear dynamics with a PWA model and then a PWA controller can be designed to stabilize the inverted pendulum.

Start with a nonlinear model of the dynamics of an inverted pendulum on a cart. With x corresponding to the position of the cart and θ the angle of the pendulum ($\theta = \pm\pi$ at the vertical position), the state was chosen to be $w = \begin{bmatrix} x_1 & x_2 & x_3 & x_4 \end{bmatrix}^T = \begin{bmatrix} x & \theta & \dot{x} & \dot{\theta} \end{bmatrix}^T$. The dynamics are then

$$\dot{w} = \begin{bmatrix} 0 & 0 & 1 & 0 \\ 0 & 0 & 0 & 1 \\ 0 & 0 & 0 & 0 \\ 0 & 0 & 0 & 0 \end{bmatrix} w + \begin{bmatrix} 0 \\ 0 \\ f_1(w) \\ f_2(w) \end{bmatrix} + \begin{bmatrix} 0 \\ 0 \\ \frac{1}{M} \\ \frac{-3}{2lM}\cos(x_2) \end{bmatrix} u,$$

$$f_1(w) = \frac{1}{M}\left(\frac{m_p l}{2} x_4^2 \sin(x_2) + \frac{3 m_p g}{8}\sin(2x_2)\right),$$

$$f_2(w) = -\frac{3}{2l}\left(g\sin(x_2) + f_1(x_2, x_3, x_4)\cos(x_2)\right),$$

$$M = m_c + m_p \left(1 - \frac{3}{4}\cos^2(x_2)\right)$$

where m_c is the mass of the cart, m_p is the mass of the pendulum, u is the force applied to the cart, l is the length of the pendulum and g is the gravitational acceleration. For this particular example, $m_p = \frac{1}{3}$ Kg, $m_c = 1$ Kg, $l = 0.2$ m and $g = 9.8\text{ms}^{-2}$.

[Figure 7 about here.]

A uniform rectangular 2D grid with four cells was generated for the neighborhood $\mathcal{D} = \left\{x \in I\!R^4 \,|\, x_2 \in \left[\frac{3\pi}{4}, \frac{5\pi}{4}\right],\, x_4 \in [-2, 2]\right\}$ of the open-loop unstable equilibrium point. In particular, the grid is specified by the x_2 values $\{\frac{3\pi}{4}, \pi, \frac{5\pi}{4}\}$ and the x_4 values $\{-2, 0, 2\}$. A piecewise-affine approximation of the nonlinear dynamics was computed using this grid. A state feedback controller was then designed using the PWA model. The closed-loop equilibrium points of all polytopic regions were placed at $x_{cl} = [\ 0 \quad \pi \quad 0 \quad 0\ ]^T$. The state and input weighting matrices for the design of the initial controller were $Q = \text{diag}([\ 10^2 \quad 10^{-5} \quad 10^{-1} \quad 2 \times 10^4\ ])$ and $R = 2 \times 10^2$ respectively. The initial controller does not verify the constraints for the avoidance of sliding modes, so one of the objectives of the design is to develop a new controller that satisfies these constraints. Furthermore, the control signals were constrained to be continuous at the boundaries of regions $\mathcal{R}_1$-$\mathcal{R}_4$ and $\mathcal{R}_6$-$\mathcal{R}_7$. The V–K iteration parameters for this problem were $l_0 = 0.1$, $l_1 = 150$, $l_2 = 150$ and $\epsilon = 0.1$. After one V–K iteration both a controller and a Lyapunov function were found that satisfied all of these objectives. The controller is described by

$$\begin{aligned}
K_1 &= [\ 1.4284 \quad -27.262 \quad 2.4829 \quad -7.3204\ ], \quad m_1 = 85.645 \\
K_2 &= [\ 1.5553 \quad -28.914 \quad 2.7034 \quad -8.2724\ ], \quad m_2 = 90.836 \\
K_3 &= [\ 1.5553 \quad -28.914 \quad 2.7034 \quad -7.9705\ ], \quad m_3 = 90.838 \\
K_4 &= [\ 1.4284 \quad -26.556 \quad 2.4829 \quad -7.3204\ ], \quad m_4 = 83.429 \\
K_5 &= K_3,\ K_6 = K_4,\ K_7 = K_1,\ K_8 = K_2, \\
m_5 &= m_3,\ m_6 = m_4,\ m_7 = m_1,\ m_8 = m_2.
\end{aligned}$$

Note that, although no symmetry was constrained in the design, the resulting controller parameters are symmetric. The Lyapunov function that proves exponential convergence of the closed-loop piecewise-affine system is shown in figure 8 and the level curves of the projection of this function onto the $x_2 - x_4$ plane are over-plotted with the trajectories of the simulations (using a piecewise-affine approximation of the plant dynamics) in figure 9. Additional trajectories of the simulations using the nonlinear plant dynamics are shown in figure 10. The controller renders the piecewise-affine closed-loop system exponentially

stable inside the largest level set contained in $\mathcal{D}$ with a guaranteed decay rate of at least $\min \alpha_i = 0.3273$.

[Figure 8 about here.]

[Figure 9 about here.]

[Figure 10 about here.]

A comparison of the simulation results of the initial and new controllers for the nonlinear plant is shown in figure 11. The figure clearly shows that the new controller provides a solution to the problem that requires a much smaller change in the cart position to equilibrate the pendulum. As discussed previously, this controller also guarantees that sliding modes will not be generated at the switching.

[Figure 11 about here.]

Example 3: This problem considers a first-order open-loop unstable plant and solves the controller synthesis problem using two of the local algorithms presented in Section 3.3. Consider a temperature exchanger system connected to a heat source with unitary flow rate $q_0 = 1$ and whose temperature obeys the first-order differential equation $\dot{T} = c(T)T + q_0 + u$. The temperature coefficient has the following piecewise-constant characteristic

$$c(T) = \begin{cases} 1 & T < 0 \\ -1 & T > 0 \end{cases}$$

which (setting $x = T$) generates the polytopic regions $\mathcal{R}_1 = \{x \in I\!R \,|\, x < 0\}$ and $\mathcal{R}_2 = \{x \in I\!R \,|\, x > 0\}$. Assume the temperature is measured but the measurement is noisy. It is then necessary to estimate the temperature to determine when to switch controllers.

An output feedback controller was designed to stabilize the open-loop unstable equilibrium point of region $\mathcal{R}_1$ at $x = -1$, which implies that $x_{cl}^1 = -1$. For region $\mathcal{R}_2$, the closed-loop equilibrium point was selected to also be located at the same position, i.e, $x_{cl}^2 = -1$. These positions for the equilibrium points yield the constraints $m_1 = 0$, and $A_2 x_{cl}^2 + b_2 + B_2 m_2 = 0$. The sliding mode constraints (23) for case 1 (with $x_c = \hat{x}$) are automatically verified given that $B_1 = B_2$ and $b_1 = b_2$. The sliding mode constraints (24) and (25) for cases 2 and 3, respectively, are $m_1 - K_1 x_{cl}^1 = m_2 - K_2 x_{cl}^2$, and $L_1 = L_2$.

The initial controller for region $\mathcal{R}_1$ was designed using LQG with state/input weighting matrix $W = \text{diag}(4, 1)$ and noise weighting matrix $V = \text{diag}\,(10^{-7}, 1)$. This controller is described by $K_1 = -3.2361$, $L_1 = 2$ and $m_1 = 0$. For region $\mathcal{R}_2$, the sliding mode constraints specify that the initial controller parameters be given by $K_2 = K_1 + 2 = -1.2361$, $L_2 = L_1$ and $m_2 = -2$.

The optimized control Lyapunov function parameters were constrained to be the same for regions $\mathcal{R}_1 \times \mathcal{R}_1$ and $\mathcal{R}_1 \times \mathcal{R}_2$ and the same for regions $\mathcal{R}_2 \times \mathcal{R}_1$ and $\mathcal{R}_2 \times \mathcal{R}_2$. Both the V–K iteration and the hybrid algorithm described in Section 3.3 were used to solve the dynamic output feedback optimization problem.

The resulting controller using the V–K iteration method (after one iteration with $l_0 = 10^{-3}$, $l_1 = l_2 = 10$ and $\epsilon = 10^{-3}$) is described by

$$K_1 = -9.9998,\ K_2 = -7.9998,\quad L_1 = L_2 = 9.9999,\ m_1 = 0,\ m_2 = -2.$$

This controller renders the closed-loop system exponentially stable inside the largest level set contained in $\mathcal{D} = \{\tilde{x} \in I\!R^2 \,|\, x \in [-20, 20]\,, \hat{x} \in [-20, 20]\}$ with a guaranteed decay rate of at least $\min_i \alpha_i = 5.7869$. The control Lyapunov function for the V–K iteration controller is shown in figure 12.

[Figure 12 about here.]

[Figure 13 about here.]

The controller obtained by the hybrid method after 96 iterations (using the same initial controller and the same constraints) is characterized by

$$K_1 = -9.9453,\ K_2 = -7.9453,\quad L_1 = L_2 = 9.5863,\ m_1 = 0,\ m_2 = -2$$

which renders the closed-loop system exponentially stable inside the largest level set contained in $\mathcal{D}$ with a guaranteed decay rate of at least $\min \alpha_i = 5.7629$. Both controllers were simulated in a feedback loop with the plant for the initial condition $x = 0.5$, $\hat{x} = -0.5$. The results are over-plotted in figure 13, where it is clear that, as expected, the convergence of the two controllers is very similar, since their parameters are very close. These results show that, at least for this particular example, the two algorithms yield very similar suboptimal solutions. However, as expected, it takes many more iterations using the hybrid method.

Starting the closed-loop system in all possible combinations (plant in $\mathcal{R}_i$ and controller in $\mathcal{R}_j$) using the V–K controller gives the results in figure 14, which shows trajectories on the

plane (x, x_c) over-plotted with the Lyapunov function level curves. Note that, as desired, all trajectories starting from within the largest region of guaranteed exponential stability for the system converge to the equilibrium point in the bottom left rectangle (which is region $(\mathcal{R}_1 \times \mathcal{R}_1)$).

[Figure 14 about here.]

Example 4: This example considers the tunnel diode circuit shown in figure 15 [Hassibi and Boyd, 1998, Rodrigues *et al.*, 2000]. With time expressed in 10^{-10} seconds, the inductor current in milliAmps and the capacitor voltage in Volts, the dynamics can be written as

$$\begin{bmatrix} \dot{x}_1 \\ \dot{x}_2 \end{bmatrix} = \begin{bmatrix} -30 & -20 \\ 0.05 & 0 \end{bmatrix} \begin{bmatrix} x_1 \\ x_2 \end{bmatrix} + \begin{bmatrix} 24 \\ -50g(x_2) \end{bmatrix} + \begin{bmatrix} 20 \\ 0 \end{bmatrix} u.$$

Following [Hassibi and Boyd, 1998], the characteristic of the tunnel diode $g(x_2)$ is defined to be the piecewise-affine function shown in figure 16 which generates the polytopic regions

$$\mathcal{R}_1 = \{x \in I\!R^2 \,|\, x_2 < 0.2\} \;, \quad \mathcal{R}_2 = \{x \in I\!R^2 \,|\, 0.2 < x_2 < 0.6\} \;, \quad \mathcal{R}_3 = \{x \in I\!R^2 \,|\, x_2 > 0.6\}$$

Assume that the measured output is the current x_1, which is not the variable that drives the switching. A nominal output feedback controller design was performed for an augmented plant with first-order actuator dynamics to globally stabilize the open-loop locally stable equilibrium point of region $\mathcal{R}_1$. The initial actuator time constant was selected as $\tau = 100$. The locations for the equilibrium points were selected at

$$x_{cl}^1 = \begin{bmatrix} 0.7059 \\ 0.1412 \end{bmatrix}, \; x_{cl}^2 = \begin{bmatrix} -0.8333 \\ 1.1167 \end{bmatrix}, \; x_{cl}^3 = \begin{bmatrix} -0.6133 \\ 0.3967 \end{bmatrix}.$$

The initial controller was then designed using LQG with $W = \text{diag}(0.1, 0.1, 1, 1)$ and $V = \text{diag}\,(10^{-7} I_{3\times 3}, 10^{-8})$. The nominal controller after 4 iterations (subject to $\epsilon = 10^{-3}$, $l_0 = 0.1$, $l_1 = l_2 = 100$, $\tau_1 = \tau_2 = \tau_3 = \tau < 1000$, all entries in the different matrices bounded between $\pm l_1$ and all sliding modes constraints) is described by

$$\begin{aligned} K_1 &= \begin{bmatrix} 1.1024, & 0.8633, & 0.0414 \end{bmatrix} , \quad m_1 = 0, \\ K_2 &= \begin{bmatrix} 0.8246 & 0.0005, & -0.2577 \end{bmatrix} , \quad m_2 = -1.333 \\ K_3 &= \begin{bmatrix} 0.8381 & -0.0002, & -0.2636 \end{bmatrix} , \quad m_3 = -1.723, \\ \tau &= 44.882 \;, \quad \min \alpha_i = 0.1196 \end{aligned}$$

$$L_1 = \begin{bmatrix} 12.548 \\ -2.9391 \\ 65.6589 \end{bmatrix}, \quad L_2 = \begin{bmatrix} 28.1906 \\ -2.9391 \\ 7.1806 \end{bmatrix}, \quad L_3 = \begin{bmatrix} 27.4955 \\ -2.9391 \\ 13.9530 \end{bmatrix}.$$

For this controller, the extended design phase consisted of a post-analysis in $\mathcal{D} = \{\tilde{x} \in \mathbb{R}^6 \mid x_2 \in [-3, 3], \hat{x}_2 \in [-3, 3]\}$. The control Lyapunov function parameters were restricted to be the same for polytopic cells where the plant state is in the same region (*e.g.,* cells $\mathcal{R}_1 \times \mathcal{R}_1$ and $\mathcal{R}_1 \times \mathcal{R}_2$ are restricted to have the same Lyapunov parameters). This post-analysis showed that the nominal controller exponentially stabilizes the closed-loop equilibrium point in the largest invariant set contained in $\mathcal{D}$ with a guaranteed decay rate of at least $\min_i \alpha_i = 0.1$. As shown in figure 17, the largest invariant set contained in $\mathcal{D}$ offers a much broader region of guaranteed exponential stability as compared to the open-loop region of stability. In particular, note that the closed-loop region of stability contains the positions of the open-loop equilibrium points of both region $\mathcal{R}_2$ and $\mathcal{R}_3$.

[Figure 15 about here.]

[Figure 16 about here.]

Starting the closed-loop system in all possible combinations (plant in $\mathcal{R}_i$ and controller in $\mathcal{R}_j$) gives the results in figure 17. The plot shows a projection of the trajectories on the (x, x_c) plane over-plotted with the Lyapunov function level curves ($x = x_2$ and $x_c = \hat{x}_2$ are the variables that drive the switching). Note that, as desired, all trajectories starting from within the largest region of guaranteed exponential stability for the system converge to the equilibrium point in the bottom left rectangle (which is region $\mathcal{R}_1 \times \mathcal{R}_1$).

[Figure 17 about here.]

[Figure 18 about here.]

5 Conclusions

This paper presents a new method for designing state and dynamic output feedback controllers for piecewise-affine systems based on mathematical programming. More specifically, the proposed technique formulates the search for a piecewise-quadratic control Lyapunov

function and a piecewise-affine control law as an optimization problem subject to linear constraints and a bilinear matrix inequality. It is well known that the synthesis of controllers for piecewise-affine systems is a computational complex problem and that, while branch and bound solution algorithms are available, these can, in worst-case, run in non-polynomial time. As a result these algorithms are typically of limited practical use for applications involving medium- to large-scale design problems. Thus, this paper focuses on obtaining sub-optimal solutions to the non-convex optimization problem using extensions of iterative algorithms available in the literature. These solution approaches execute efficient polynomial-time algorithms at each step of the iteration and provide (sub-optimal) controller solutions that yield good closed-loop performance. Three such solution algorithms were presented and two of these were shown to converge to very similar control solutions for an output feedback design problem. For the four examples in the paper, algorithm #1 was shown to require less than five iterations to yield controllers that exponentially stabilize the systems and obtain good performance in the (nonlinear) simulations.

The paper also shows that a stabilizing regulator and observer can be designed to guarantee the absence of sliding modes in the switching of a piecewise-affine system. A key result of this work is that the controllers are designed to enable switching based on state estimates rather than on measured outputs. Furthermore, the controllers guarantee that the closed-loop piecewise-affine system is either asymptotically or exponentially stable. The inputs to the design process are the dynamics of the PWA plant, the parameters of the polytopic description and the desired closed-loop equilibrium points for each polytopic region. Given a nonlinear dynamical system, all these inputs are provided by the algorithm developed in [Rodrigues and How, 2001]. Therefore, together with that work, the results from this paper enable a fully automated design of controllers for any simplicial piecewise-affine approximation of a nonlinear system in the class described in [Rodrigues and How, 2001]. The entire process has been codified in a Matlab toolbox.

References

[Andronov and Chaikin, 1949] Andronov, A. and Chaikin, C. (1949). *Theory of Oscillations*. Princeton University Press, Princeton, New Jersey.

[Banjerdpongchai and How, 2000] Banjerdpongchai, D. and How, J. P. (2000). Parametric robust H_2 control design using LMI synthesis. *AIAA Journal Guidance, Control, and Dynamics*, 23(1):138–142.

[Bemporad *et al.*, 2000] Bemporad, A., Borrelli, F., and Morari, M. (2000). Optimal con-

trollers for hybrid systems: stability and piecewise linear explicit form. In *Proceedings of the 39th IEEE Conference on Decision and Control*, pp. 1810–1815.

[Bemporad and Morari, 1999] Bemporad, A. and Morari, M. (1999). Control of systems integrating logic, dynamics, and constraints. *Automatica*, 35(3):407–427.

[Blondel and Tsitsiklis, 1999] Blondel, V. D. and Tsitsiklis, J. N. (1999). Complexity of stability and controllability of elementary hybrid systems. *Automatica*, 35(3):479–489.

[Bokhoven, 1981] Bokhoven, W. G. V. (1981). *Piecewise Linear Modelling and Analysis*. Kluwer Techische Boeken, Deventer, the Netherlands.

[Boyd *et al.*, 1994] Boyd, S., Ghaoui, L. E., Feron, E., and Balakrishnan, V. (1994). *Linear Matrix Inequalities in System and Control Theory*, volume 15 of *Studies in Applied Mathematics*. SIAM.

[Branicky, 1996] Branicky, M. S. (1996). General hybrid dynamical systems: Modeling, analysis, and control. In Alur, R., Henzinger, T., and Sontag, E. D., editors, *Hybrid Systems III Verification and Control: Lecture Notes in Computer Science*, volume 1066, pp. 186–200. Springer-Verlag, Berlin.

[Chua, 1977] Chua, L. (1977). Section-wise piecewise linear functions. canonical representation, properties and applications. *Proceedings of the IEEE*, 65:915–929.

[DeCarlo *et al.*, 2000] DeCarlo, R. A., Branicky, M. S., Petterson, S., and Lennartson, B. (2000). Perspectives and results on the stability and stabilizability of hybrid systems. *Proceedings of the IEEE*, 88(7):915–929.

[Ferrari-Trecate *et al.*, 2000] Ferrari-Trecate, G., Mignone, D., and Morari, M. (2000). Moving horizon estimation for hybrid systems. In *Proceedings of the American Control Conference*, pp. 1684–1688.

[Goh *et al.*, 1994] Goh, K. C., Ly, J. H., Turand, L., and Safonov, M. G. (1994). Biaffine matrix inequality properties and computational methods. In *Proceedings of the American Control Conference*, pp. 850–855.

[Gonçalves *et al.*, 2001] Gonçalves, J. M., Megretski, A., and Dahleh, M. A. (2001). Global stability of relay feedback systems. *IEEE Transactions on Automatic Control*, 46(4):550–562.

[Hassibi and Boyd, 1998] Hassibi, A. and Boyd, S. P. (1998). Quadratic stabilization and control of piecewise-linear systems. In *Proceedings of the American Control Conference*, pp. 3659–3664.

[Hassibi *et al.*, 1999a] Hassibi, A., Boyd, S. P., and How, J. P. (1999a). A class of lyapunov functionals for analyzing hybrid dynamical systems. In *Proceedings of the American Control Conference*, pp. 2455–2460.

[Hassibi *et al.*, 1999b] Hassibi, A., How, J., and Boyd, S. (1999b). A path-following method for solving bmi problems in control. In *Proceedings of the American Control Conference*,

pp. 1385–1389.

[Imsland *et al.*, 2001] Imsland, L., Slupphaug, O., and Foss, B. (2001). Piecewise affine observer based robust controllers for constrained nonlinear systems. In *European Control Conference*, pp. 1876–1881.

[Johansson, 1999] Johansson, M. (1999). *Piecewise Linear Control Systems*. PhD thesis, Lund Institute of Technology.

[Johansson and Rantzer, 1998a] Johansson, M. and Rantzer, A. (1998a). Computation of piecewise quadratic lyapunov functions for hybrid systems. *IEEE Transactions on Automatic Control*, 43(4):555–559.

[Johansson and Rantzer, 2000] Johansson, M. and Rantzer, A. (2000). Piecewise linear quadratic optimal control. *IEEE Transactions on Automatic Control*, 45(4):629–637.

[Julián, 1999] Julián, P. (1999). *A High Level Canonical Piecewise Linear Representation Using a Simplicial Partition: Theory and Applications*. PhD thesis, Universidad Nacional del Sur, Argentina.

[Kalman, 1954] Kalman, R. (1954). Phase-plane analysis of automatic control systems with nonlinear gain elements. *Transactions of AIEE Part II: Applications and Industry*, 73:383–390.

[Kantner, 1997] Kantner, M. (1997). Robust stability of piecewise linear discrete time systems. In *Proceedings of the American Control Conference*, pp. 1241–1245.

[Nesterov and Nemirovsky, 1994] Nesterov, Y. and Nemirovsky, A. (1994). *Interior-point polynomial methods in convex programming*, volume 13 of *Studies in Applied Mathematics*. SIAM.

[Paré *et al.*, 2001] Paré, T., Hassibi, A., and How, J. P. (2001). A kyp lemma and invariance principle for systems with multiple hysteresis nonlinearities. *International Journal of Control*, 74(11):1140–1157.

[Peleties and DeCarlo, 1991] Peleties, P. and DeCarlo, R. A. (1991). Asymptotic stability of m-switched systems using lyapunov-like functions. In *Proceedings of the American Control Conference*, pp. 1679–1684.

[Pettersson, 1999] Pettersson, S. (1999). *Analysis and Design of Hybrid Systems*. PhD thesis, Chalmers University of Technology.

[Pettit, 1995] Pettit, N. B. O. L. (1995). *Analysis of Piecewise Linear Dynamical Systems*. Research Studies Press Ltd./ John Wiley & Sons Limited.

[Popov, 1961] Popov, V. (1961). Absolute stability of nonlinear systems of automatic control. *Automation and Remote Control*, 22:857–875.

[Rodrigues *et al.*, 2000] Rodrigues, L., Hassibi, A., and How, J. (2000). Output feedback controller synthesis for piecewise-affine systems with multiple equilibria. In *Proceedings of the American Control Conference*, pp. 1784–1789.

[Rodrigues and How, 2001] Rodrigues, L. and How, J. (2001). Automated control design for a piecewise-affine approximation of a class of nonlinear systems. In *Proceedings of the American Control Conference*, pp. 3189–3194.

[Rugh and Shamma, 2000] Rugh, W. and Shamma, J. S. (2000). Research on gain scheduling. *Automatica*, 36(9):1401–1425.

[Schutter and Moor, 1999] Schutter, B. D. and Moor, B. D. (1999). The extended linear complementarity problem and the modeling and analysis of hybrid systems. In Antsaklis, P., Kohn, W., Lemmon, M., Nerode, A., and Sastry, S., editors, *Hybrid Systems V Verification and Control: Lecture Notes in Computer Science*, volume 1567, pp. 70–85. Springer-Verlag.

[Schwartz, 1953] Schwartz, J. W. (1953). Piecewise linear servomechanisms. *Transactions of AIEE*, 72:401–405.

[Sluphaug, 1999] Sluphaug, O. (1999). *On robust constrained nonlinear control and hybrid control: BMI and MPC based state-feedback schemes*. PhD thesis, Norwegian University of Science and Technology.

[Sontag, 1981] Sontag, E. D. (1981). Nonlinear regulation: The piecewise linear approach. *IEEE Transactions on Automatic Control*, 26(2):346–358.

[Sworder and Boyd, 1999a] Sworder, D. D. and Boyd, J. E. (1999a). Control of linear jump systems in noise. *Automatica-Oxford*, 35(2):293–300.

[Sworder and Boyd, 1999b] Sworder, D. D. and Boyd, J. E. (1999b). *Estimation Problems in Hybrid Systems*. Cambridge University Press.

[Utkin, 1992] Utkin, V. I. (1992). *Sliding modes in control and optimization*. Springer Verlag, Heidelberg.

[Wu and Boyd, 2000] Wu, S.-P. and Boyd, S. (2000). SDPSOL: A Parser/Solver for Semidefinite Programming and Determinant Maximization Problems with Matrix Structure., Chapter 2 of *Recent Advances in LMI Methods for Control*, L. El Ghaoui and S.-I. Niculescu Editors, SIAM, 2000.

List of Figures

1 Polytopic regions $\mathcal{R}_i$, $\mathcal{R}_j$ and boundary 35

2 Controller Design Concept 36

3 Lyapunov Function (Example 1) 37

4 Level Curves (Example 1) 38

5 Time Response for $\psi_0 = -1.8$, $r_0 = 0$ rad/sec, $y_0 = 5$ m 39

6 Time Response for $\psi_0 = -1.8$, $r_0 = 0$ rad/sec, $y_0 = 5$ m 40

7 $x - y$ trajectory for $\psi_0 = -1.8$, $y_0 = 5$ m 41

8 Lyapunov Function (Example 2) 42

9 Level Curves and Trajectories of PWA System (Example 2) 43

10 Level Curves and Trajectories of Nonlinear System (Example 2) 44

11 Comparison of initial and V–K controller (Example 2) 45

12 Lyapunov Function (Example 3) 46

13 Convergence of Final Controllers (Example 3) 47

14 Convergence of the trajectories for initial conditions in all possible regions $\mathcal{R}_i \times \mathcal{R}_j$ (Example 3) 48

15 Circuit for Example 4. 49

16 Tunnel Diode Characteristic for Example 4. 50

17 Convergence of the trajectories for initial conditions in all possible regions $\mathcal{R}_i \times \mathcal{R}_j$ 51

18 Lyapunov Function (Example 4) 52

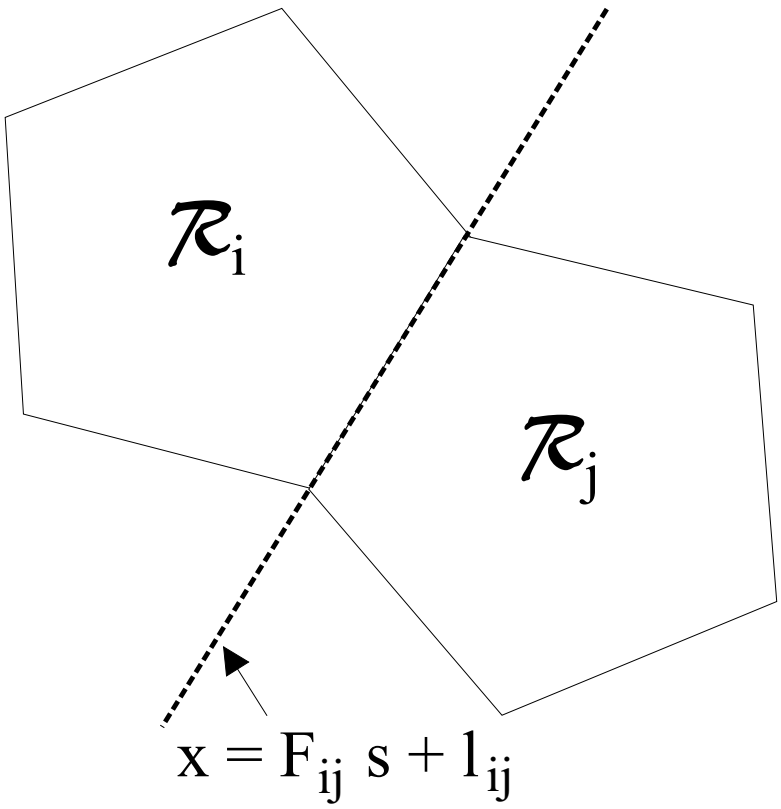

Figure 1: Polytopic regions $\mathcal{R}_i$, $\mathcal{R}_j$ and boundary

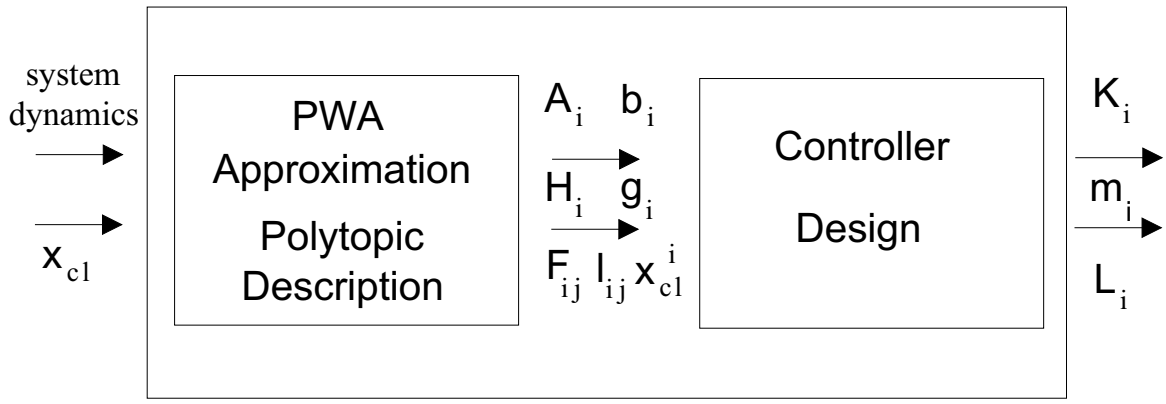

Figure 2: Controller Design Concept

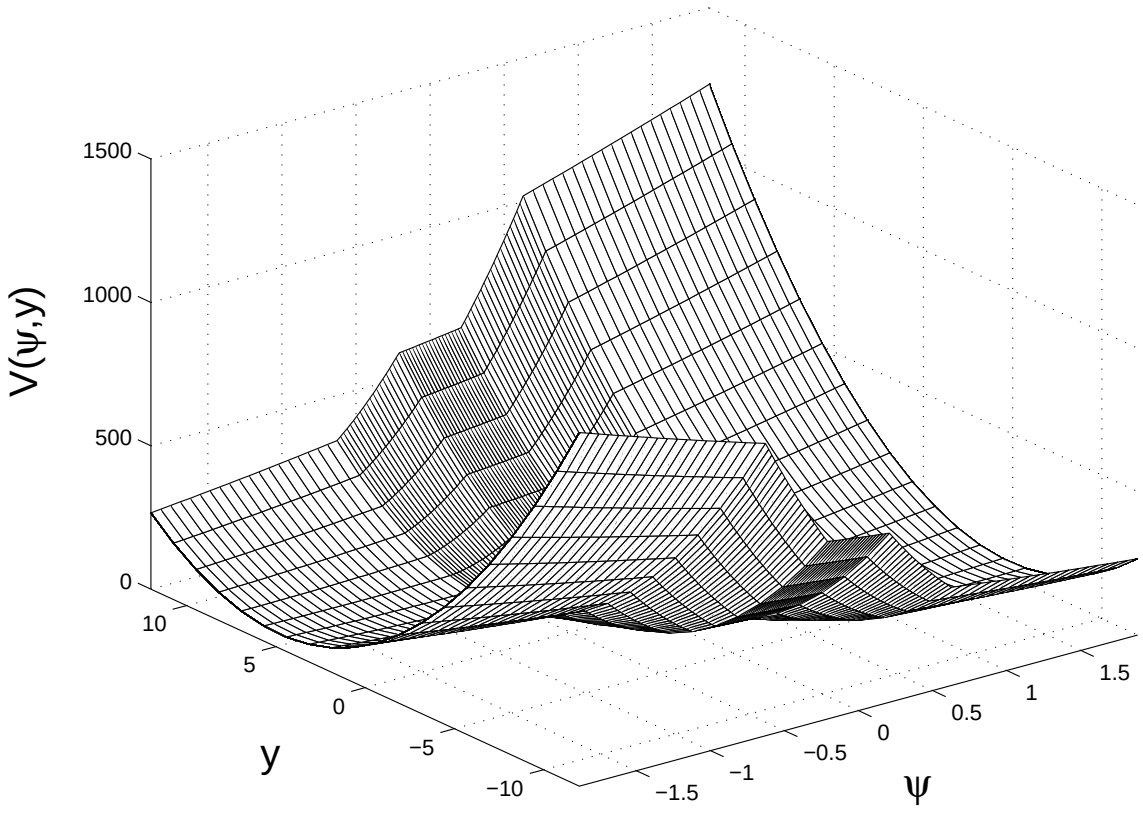

Figure 3: Lyapunov Function (Example 1)

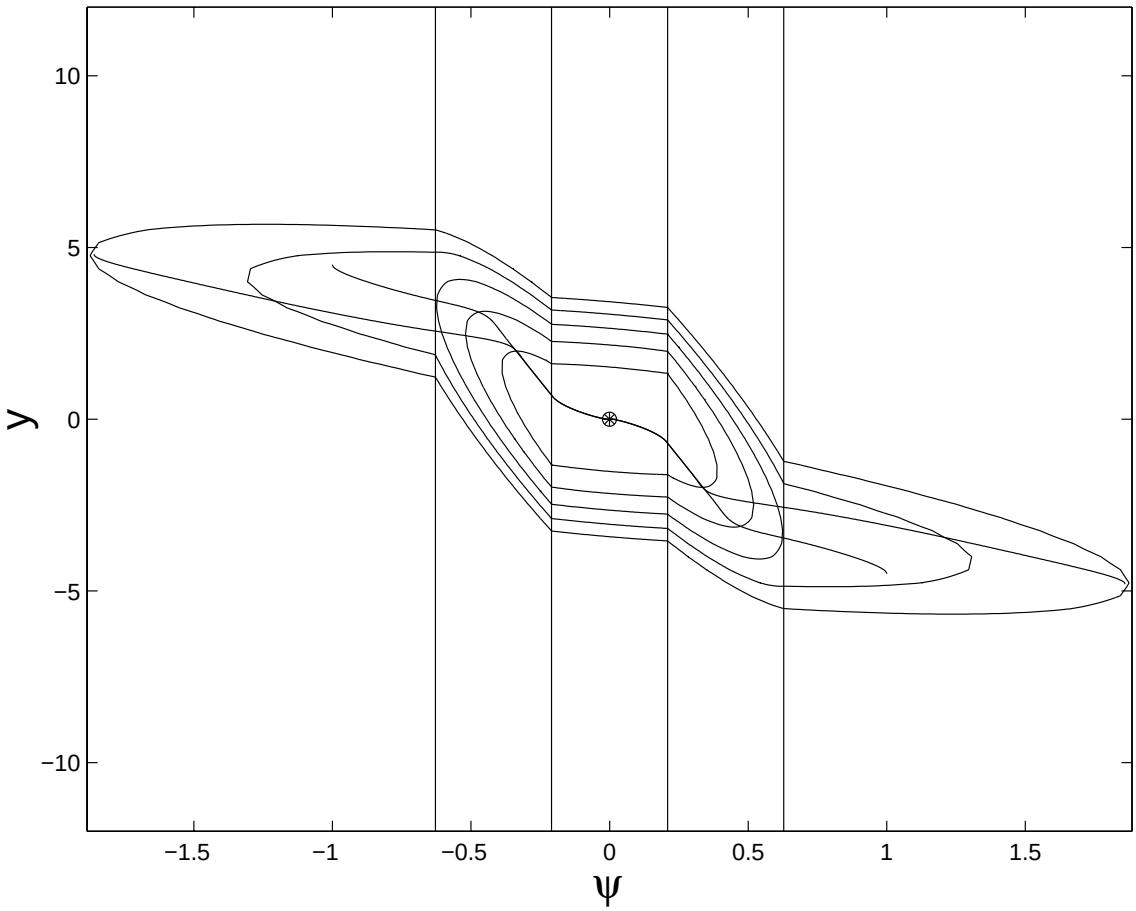

Figure 4: Level Curves (Example 1)

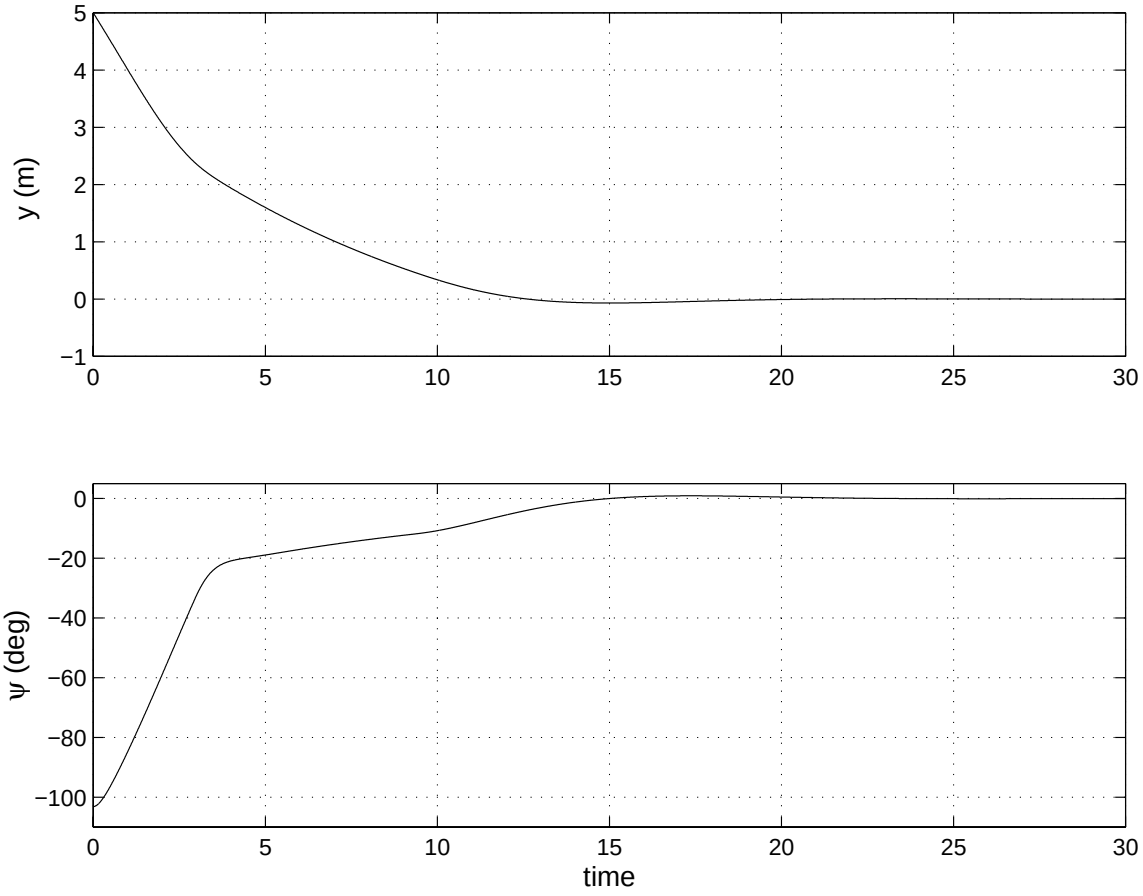

Figure 5: Time Response for $\psi_0 = -1.8$, $r_0 = 0$ rad/sec, $y_0 = 5$ m

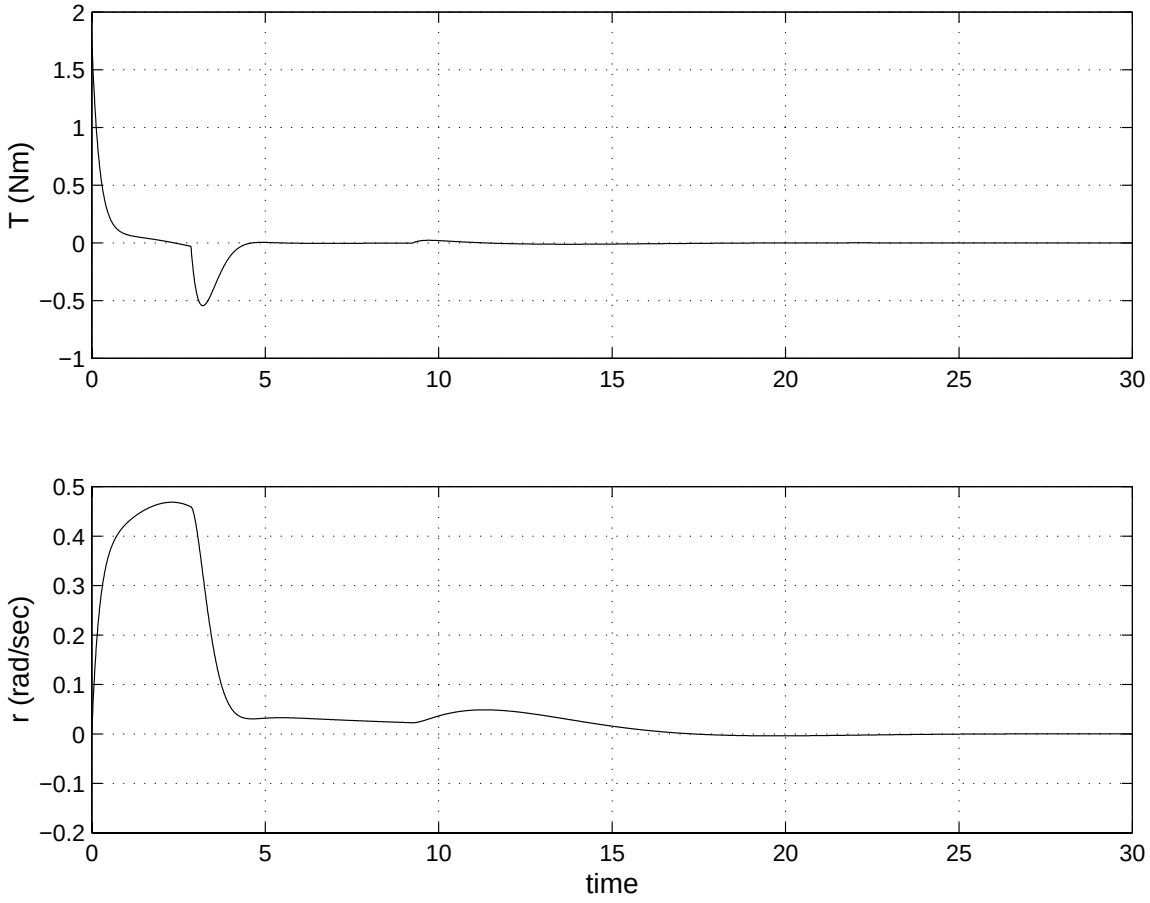

Figure 6: Time Response for $\psi_0 = -1.8$, $r_0 = 0$ rad/sec, $y_0 = 5$ m

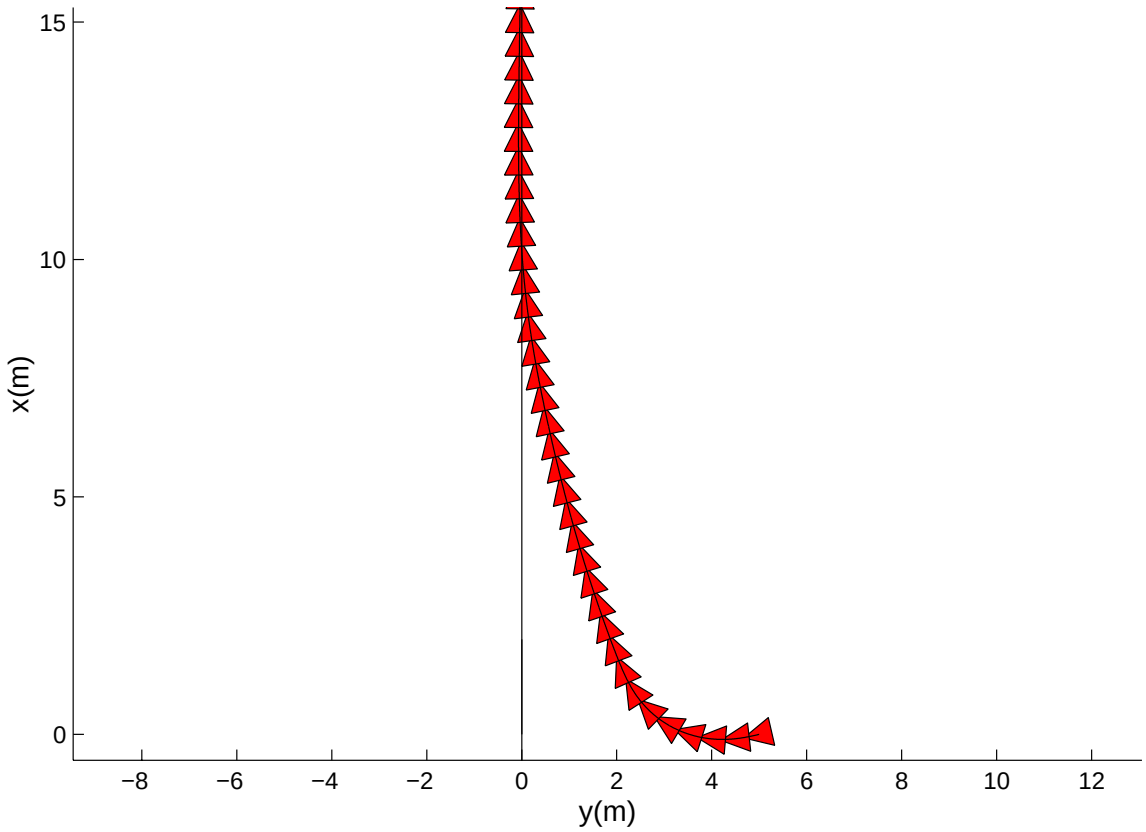

Figure 7: $x - y$ trajectory for $\psi_0 = -1.8$, $y_0 = 5$ m

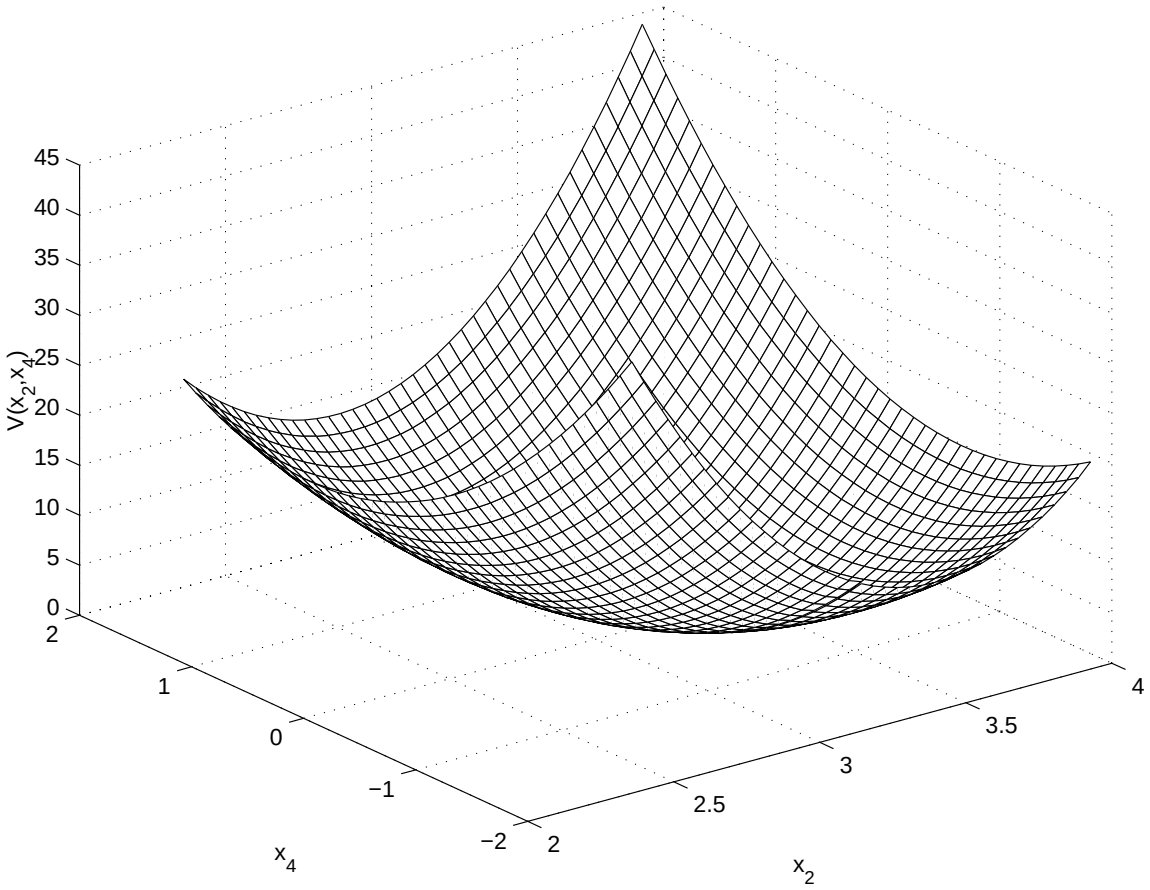

Figure 8: Lyapunov Function (Example 2)

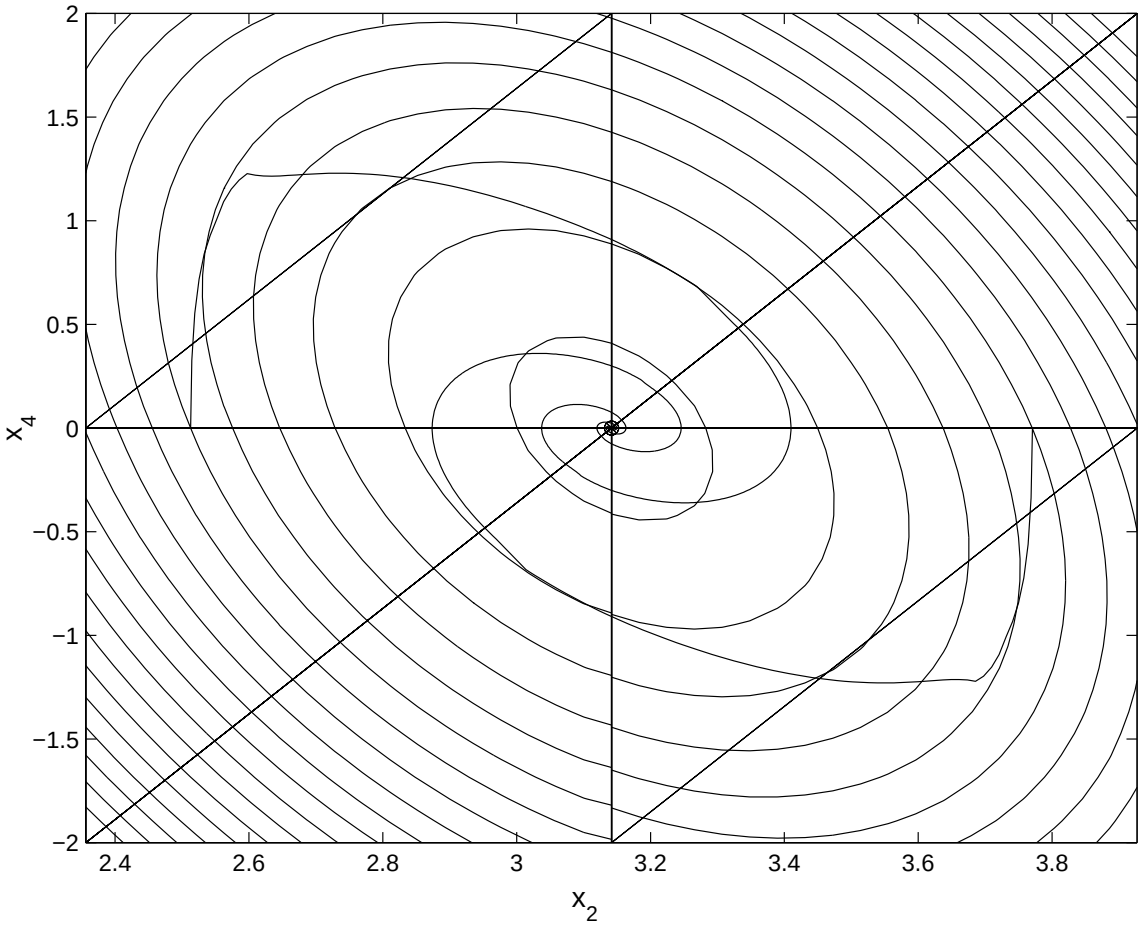

Figure 9: Level Curves and Trajectories of PWA System (Example 2)

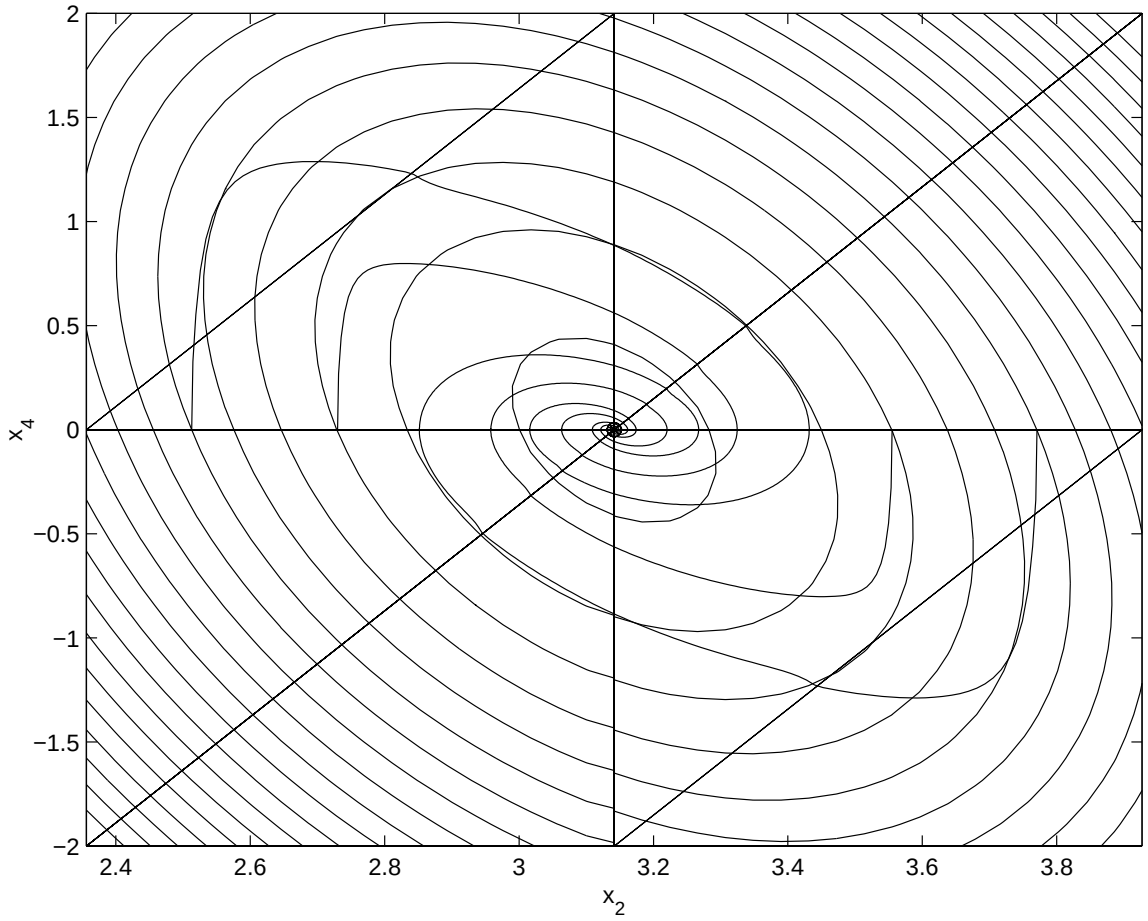

Figure 10: Level Curves and Trajectories of Nonlinear System (Example 2)

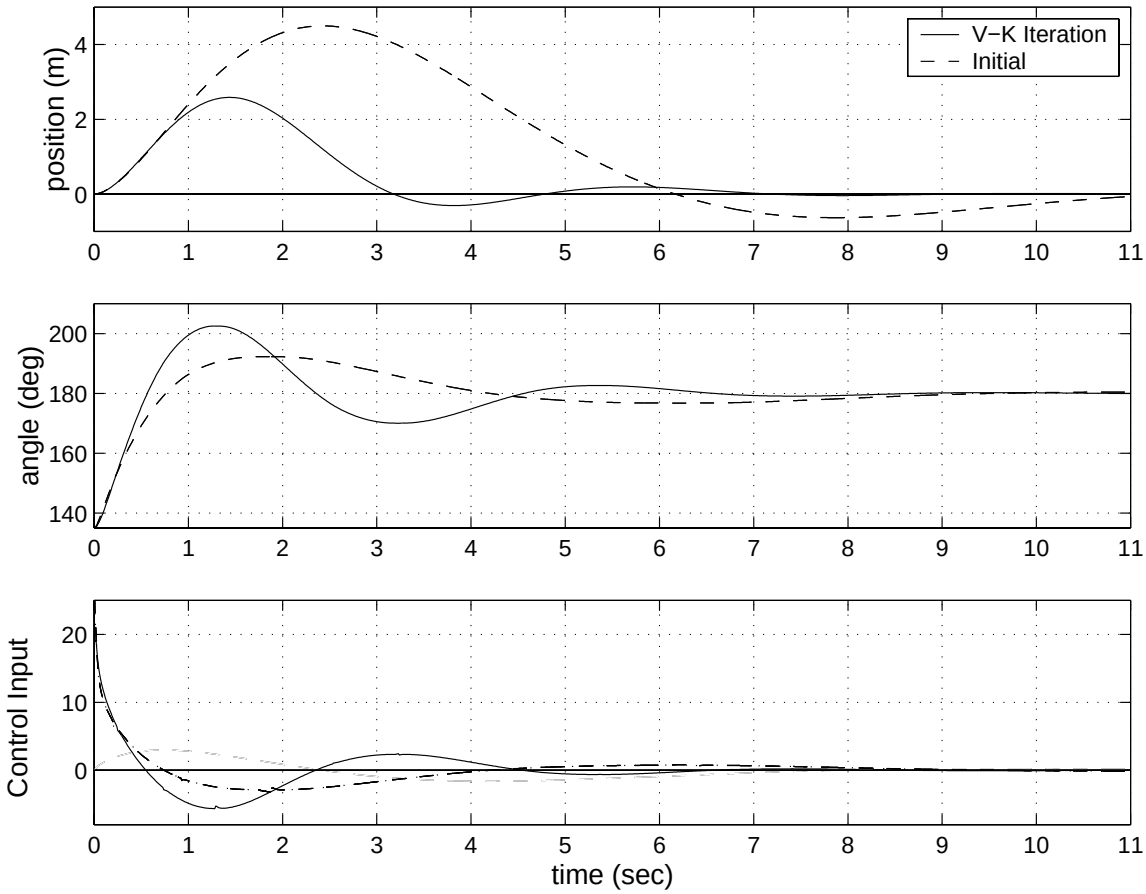

Figure 11: Comparison of initial and V–K controller (Example 2)

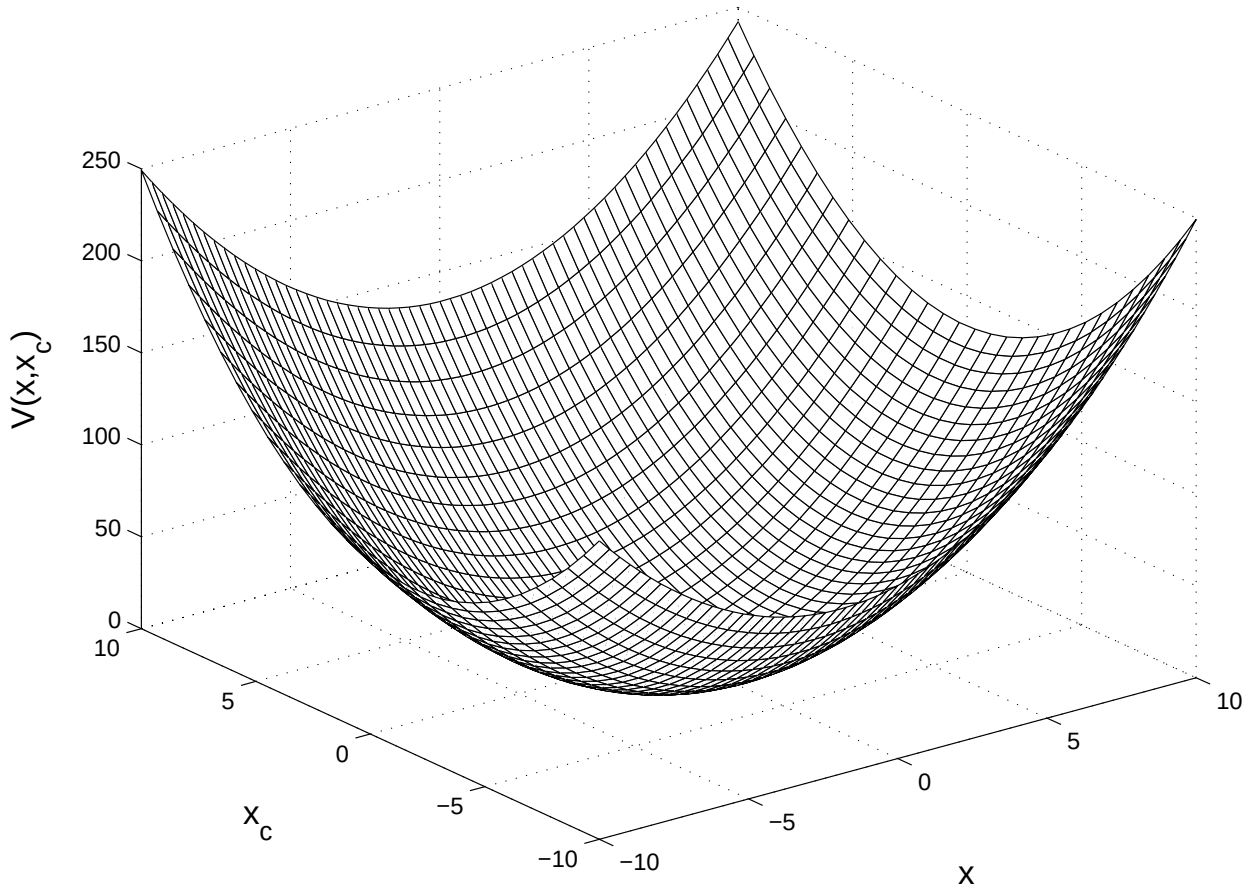

Figure 12: Lyapunov Function (Example 3)

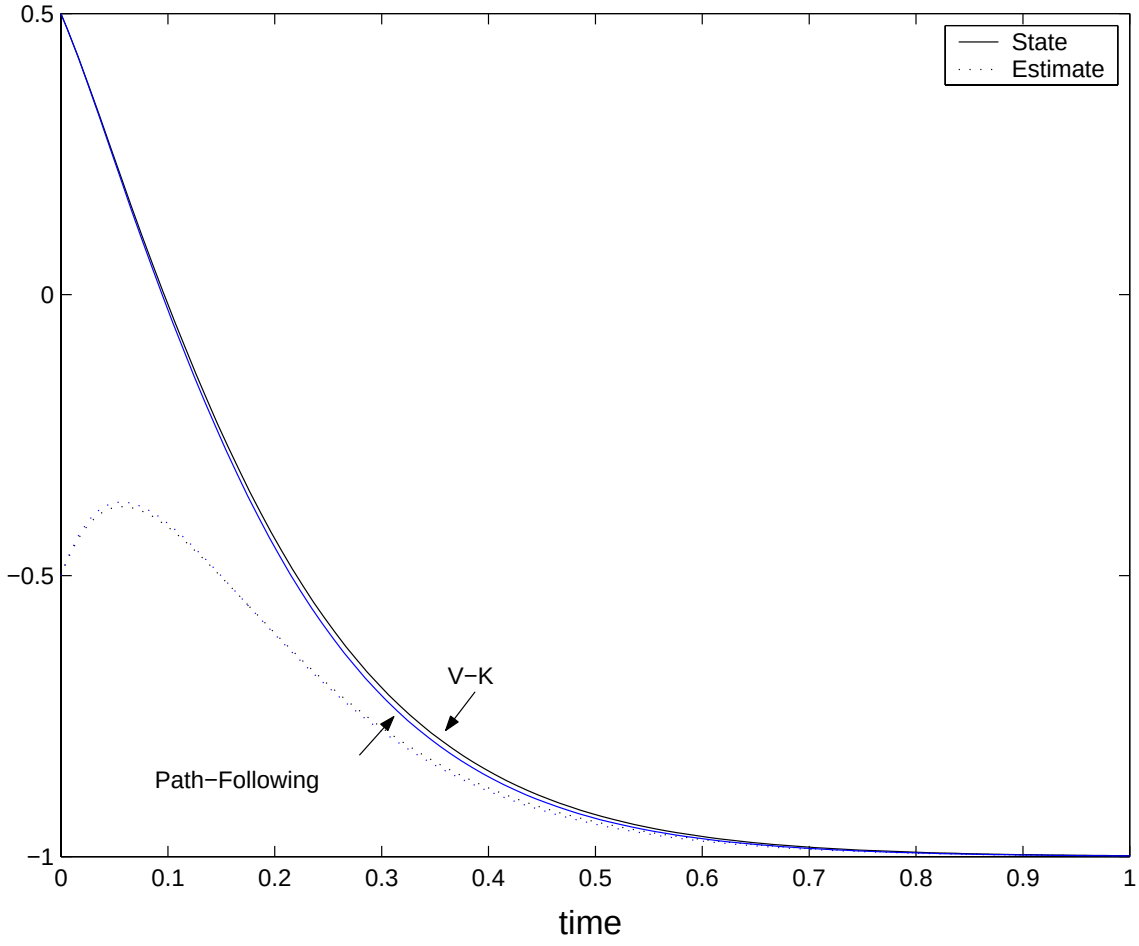

Figure 13: Convergence of Final Controllers (Example 3)

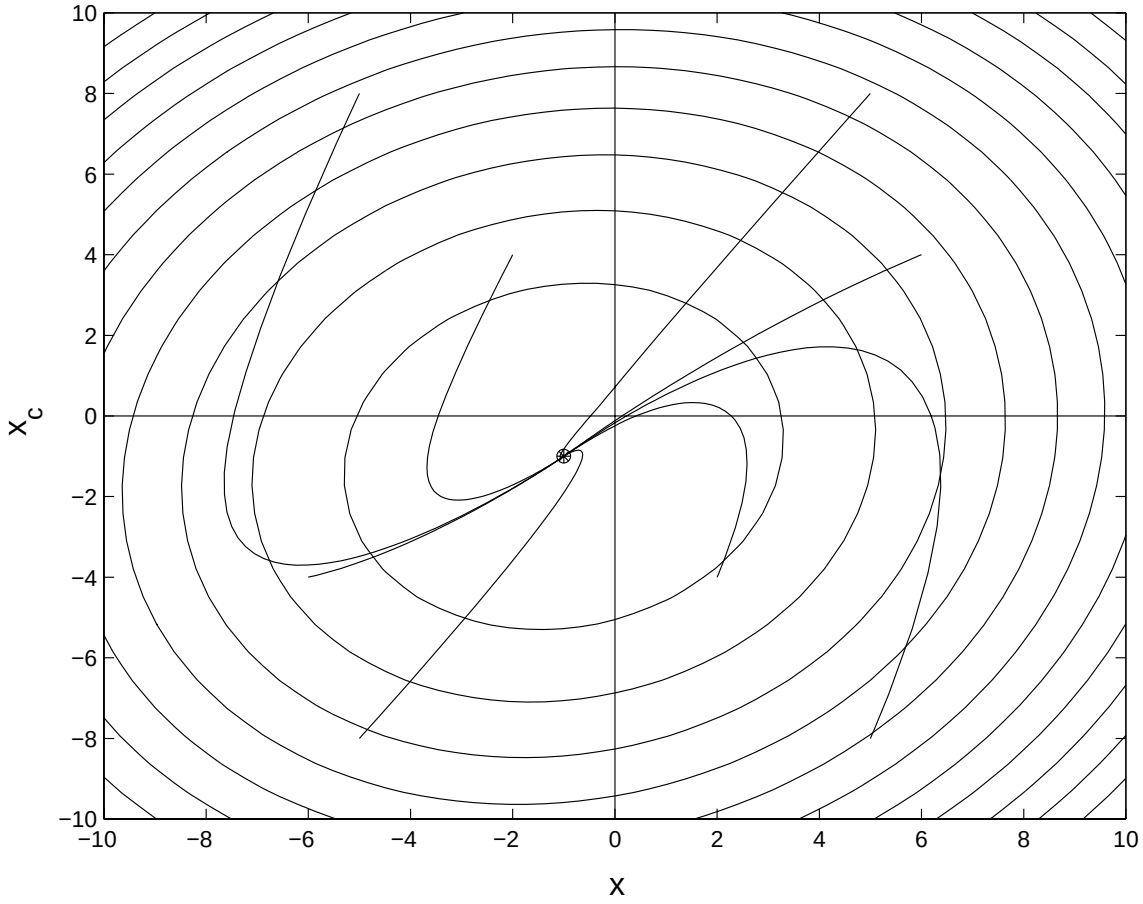

Figure 14: Convergence of the trajectories for initial conditions in all possible regions $\mathcal{R}_i \times \mathcal{R}_j$ (Example 3)

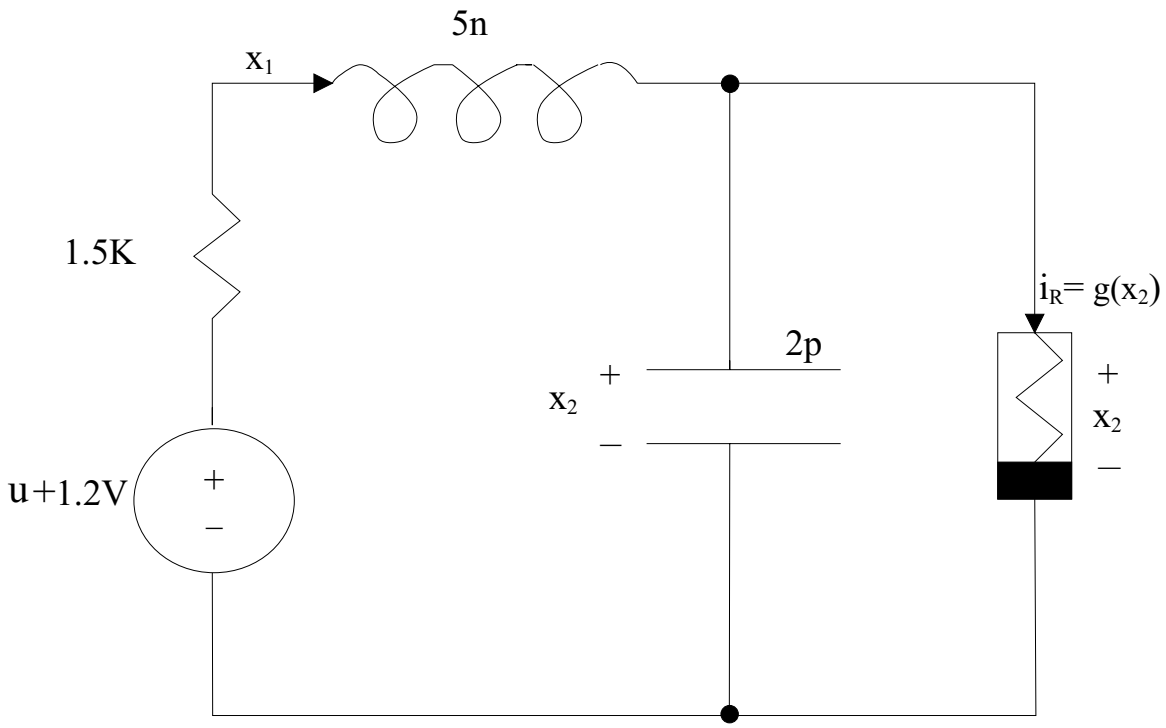

Figure 15: Circuit for Example 4.

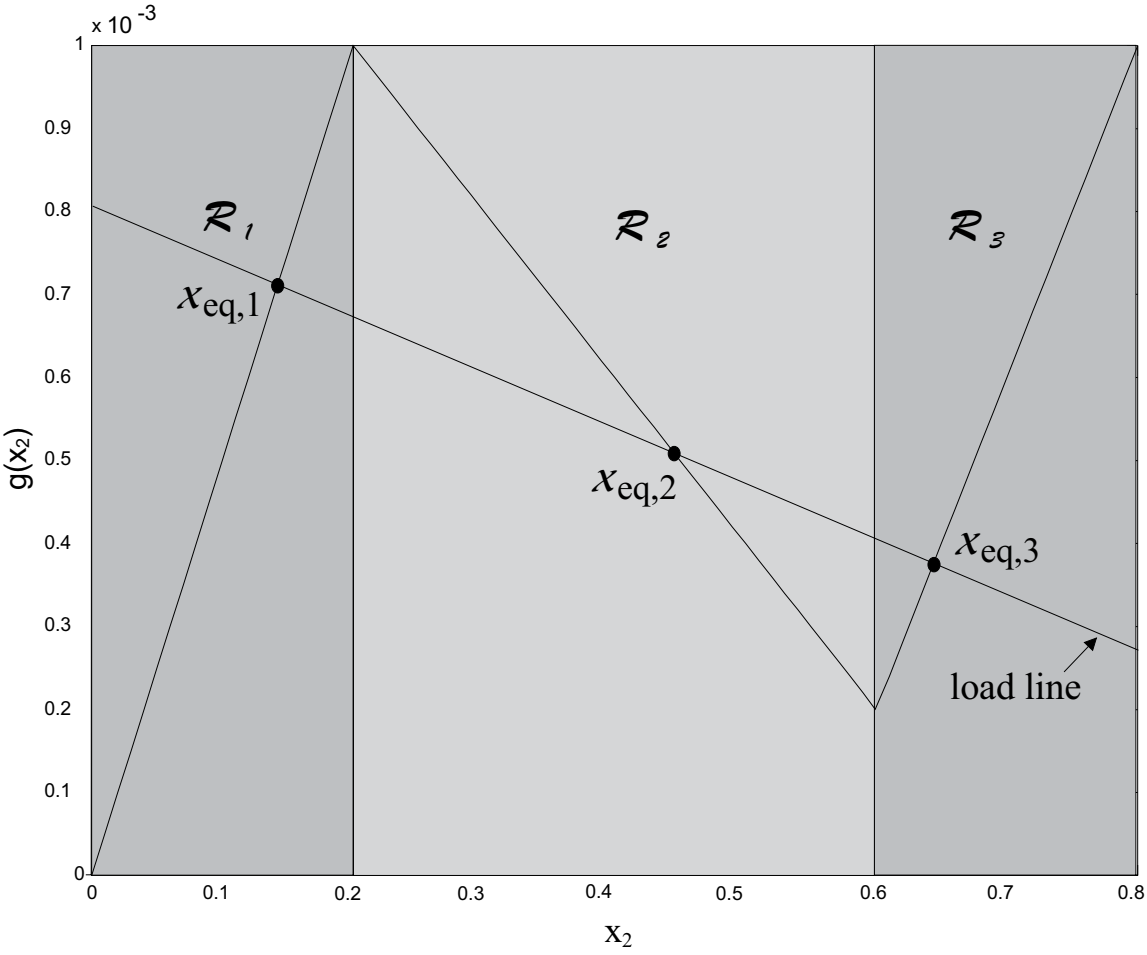

Figure 16: Tunnel Diode Characteristic for Example 4.

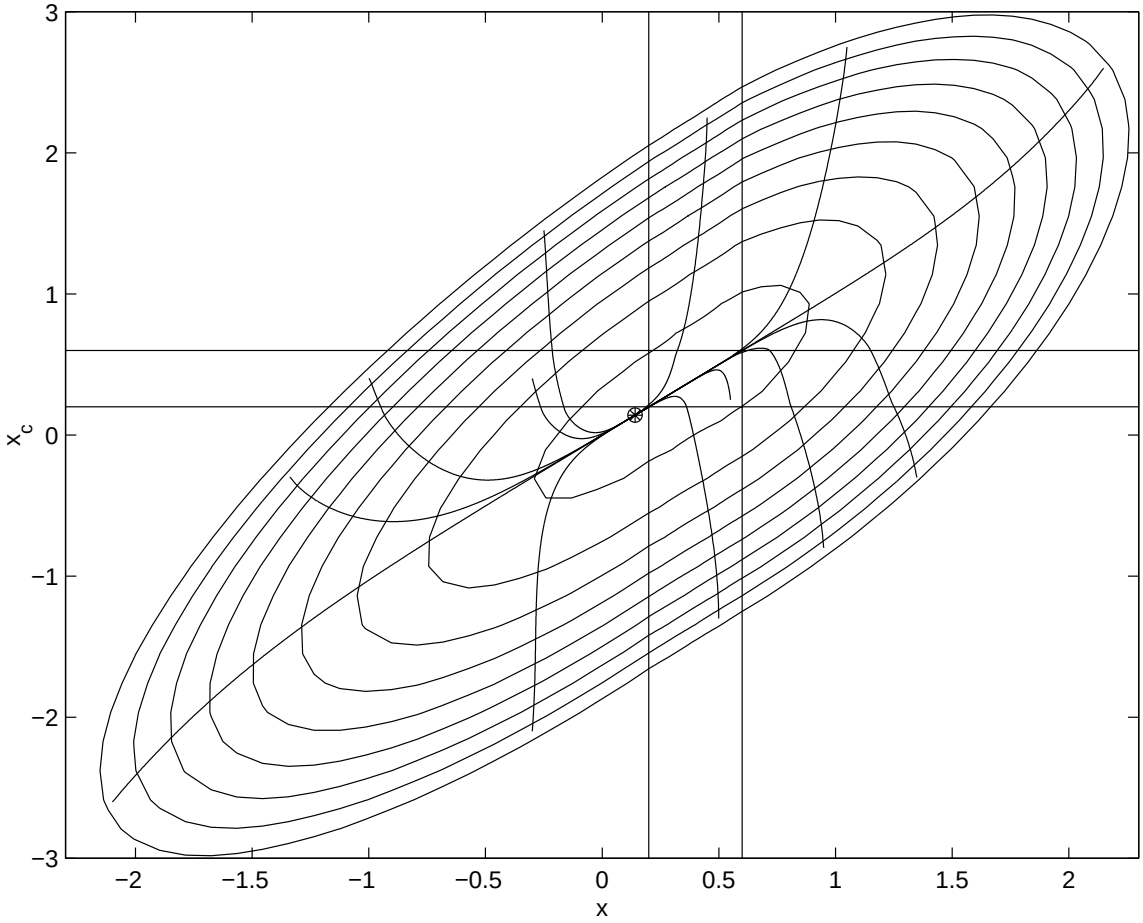

Figure 17: Convergence of the trajectories for initial conditions in all possible regions $\mathcal{R}_i \times \mathcal{R}_j$

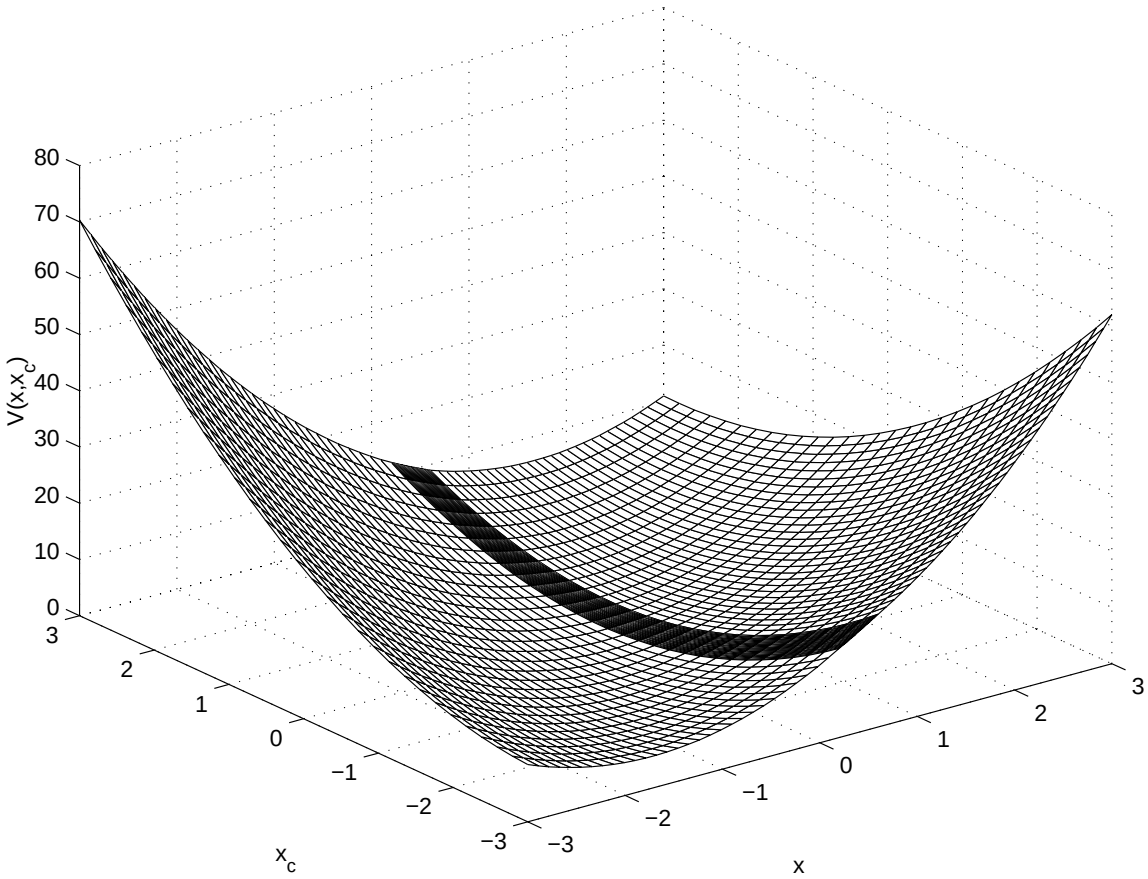

Figure 18: Lyapunov Function (Example 4)